JET–P(99)08

T T C Jones et al

Tritium Operation of the JET Neutral Beam Systems

JET–P(99)08

Tritium Operation of the JET Neutral Beam Systems

T T C Jones, A J Bickley, C D Challis, D Ciric, S J Cox, H P L de Esch[1], H-D Falter, D J Godden, D Martin, D Stork, S L Svensson[1], M J Watson, D Young.

JET Joint Undertaking, Abingdon, Oxfordshire, OX14 3EA,
[1]Present address: DRFC CEA Cadarache, F13108 Saint Paul lez Durance CEDEX, France.

Preprint of a Paper to be submitted for publication in
Fusion Engineering and Design

March 1999

ABSTRACT

Neutral Beam Injection (NBI) is a very flexible auxiliary heating method for tokamak plasmas, capable of being efficiently coupled to the various plasma configurations required in the Deuterium-Tritium Experimental campaign (DTE1) undertaken in the JET device during 1997. In particular, experiments for high fusion yield and amplification factor Q require intense NBI heating, and for maximum performance and optimum fuel mixture control in D-T plasmas it was necessary to operate the JET NBI systems in both deuterium and tritium. All technical aspects of the modifications to the JET NBI systems for compatibility with tritium operation are discussed, and the associated commissioning is described, including preparatory commissioning using deuterium. Problems experienced and their resolution are highlighted. Some specific beamline physics issues relating to tritium operation are discussed in detail, in particular experimental measurements of beam-target D-T reactions occurring in beam-stopping elements and associated modelling of isotope exchange in these components. Data on NBI performance and tritium usage and recovery for the DTE1 campaign are presented.

1. INTRODUCTION

One of the principal objectives of the JET [1] programme to the end of 1999 was to carry out experiments using Deuterium-Tritium (D-T) plasmas in an ITER-like configuration in order to provide a firm basis for the D-T operation of ITER. The first phase of D-T experiments, denoted DTE1, was conducted during 1997. The broad objectives included the demonstration of significant D-T fusion power production, the study of α-particle heating effects, and determination of isotopic dependence of the High-confinement mode (H-mode) enhancement parameter and power threshold in reactor-like plasmas. Neutral Beam Injection (NBI) of energetic hydrogenic atoms has proved to be the most flexible auxiliary heating method for tokamak plasmas, suitable for all configurations and plasma operating regimes [2]. In particular, discharges with intense predominant NBI heating in present tokamaks such as JET, in which the main power flow is via the plasma ion species, enter the hot-ion regime ($T_i >> T_e$) and in combination with enhanced plasma confinement (ELM-free H-mode or Internal Transport Barrier) maximise the achievable fusion yield and amplification factor Q. Extensive experience in such regimes had been obtained in deuterium plasmas with deuterium NBI prior to DTE1 [3]. NBI provides the dominant particle fuelling source in the plasma core, and the need to control the D:T plasma mixture therefore dictated the use of both deuterium and tritium neutral beams. The ability of NBI to provide an efficient means of tritium fuelling of the plasma core as the sole tritium particle source was first demonstrated in the JET Preliminary Tritium Experiment (PTE) [4] at low tritium plasma concentration (<10%). In DTE1, tritium gas fuelling was also used extensively [5], and it was expected (and eventually demonstrated [6]) that due to competing fuelling from particle recycling, a combination of wall loading, gas fuelling and both D^0 and T^0 NBI would all be necessary in order to maintain the optimum D:T mix in the plasma.

An advantage of operating the NB injectors in tritium is the increase of available power resulting from the improved neutralisation efficiency at the lower energy per nucleon. A further advantage specific to one of the two JET beamlines is that its triode accelerators are configured for 140kV, 30A in deuterium whilst the power supplies are rated for 160kV, 30A per beam. For minimum beam divergence using a given accelerator, the condition $I_{ext}/V_{acc}^{3/2} = \rho_{opt}$ must obtain (where I_{ext} and V_{acc} are the extracted beam current and total acceleration voltage respectively and ρ_{opt} is known as the *optimum perveance*). For hydrogenic beams consisting of similar fractions of atomic, diatomic and triatomic ions, $\rho_{opt} \propto A_g^{-1/2}$ where A_g is the atomic number of the isotope being used. The *perveance matched* condition corresponds to 160kV/30A in tritium and therefore full exploitation of the installed power capability of the HV supply was possible on this beamline in tritium. The other beamline was fitted with tetrode accelerators configured for 80kV/60A operation in deuterium, but normally operated at up to 80kV/55A. The two types of neutral injector will therefore be referred to as the 80kV and 140/160kV systems throughout the present work.

Table 1: Theoretical maximum neutral beam power and plasma fuelling rates for various beam parent gases and acceleration voltages on the JET beamlines

Species	Acceleration voltage (kV)	Current (A)	Power (MW)		Fuelling rate ($10^{20}s^{-1}$)	
			1 PINI	8 PINIs	1 PINI	8 PINIs
H_2	70	60	0.90	7.2	1.1	8.8
D_2	80	60	1.8	14	1.8	14
T_2	80	49	1.9	15	1.9	15
H_2	110	30	0.40	3.2	0.50	4.0
D_2	140	30	0.95	7.6	0.65	5.2
T_2	160	30	1.5	12	0.79	6.3

The theoretical maximum neutral beam power and particle fuelling rates delivered to the plasma for each JET neutral injector system operating in all the isotopes of hydrogen is summarised in Table 1. Both systems were modified for compatibility with tritium operation in preparation for DTE1. This involved a number of mostly minor design changes to the beamlines (such as use of all-metal seals, provision of pumped interspaces, etc.) [7]. These modifications are highlighted in Fig.1 which also provides an overview of the main beamline mechanical components. Each injector is equipped with eight plasma source and accelerator modules known as Positive Ion Neutral Injectors (PINIs) of similar configuration (either 80kV or 140/160kV) arranged in four pairs or “quadrants” with each pair sharing a common deflection magnet [8]. The most extensive system modification was the implementation of a Tritium-Deuterium Gas Introduction System (TDGIS), supplied from the central Active Gas Handling System (AGHS) [9], delivering gas via a single ground-potential inlet on each PINI [10]. This avoided use of the

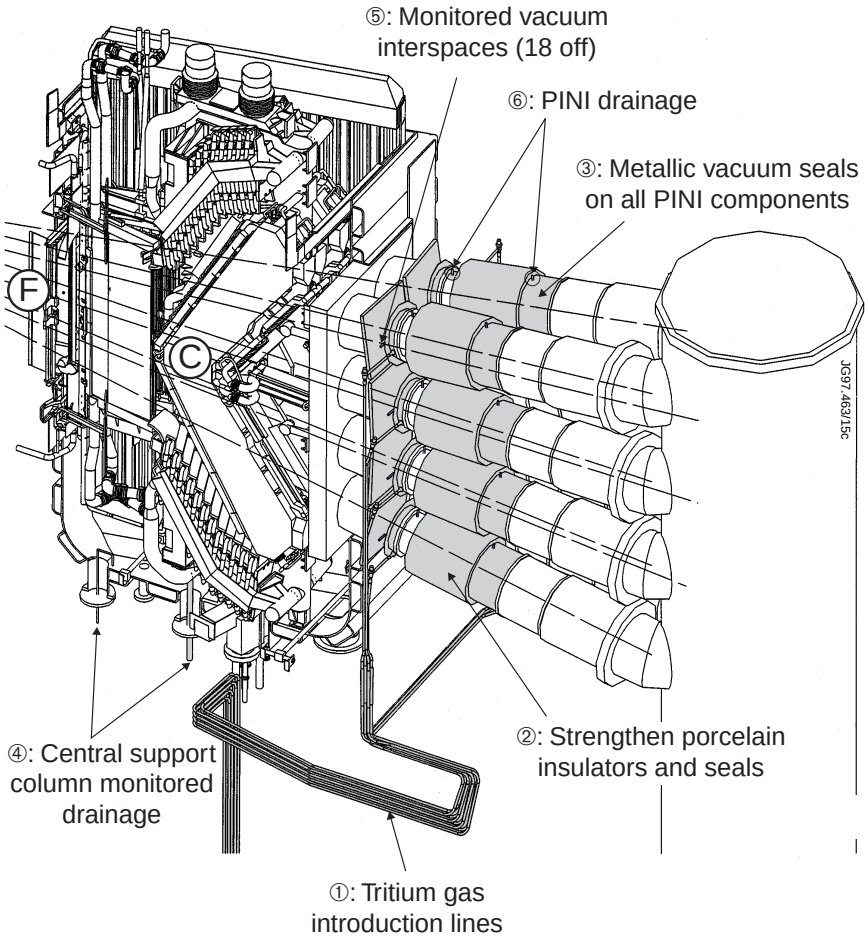

Fig.1: JET Neutral Beam Injector cutaway diagram showing the principal components and modifications required for tritium operation. 'C' denotes the central column assembly which carries the residual ion deflection magnets and ion dumps. 'F' denotes the fast shutter mechanism which was taken out of service at the start of DTE1

frangible glass insulating break in the conventional ion-source gas feed. The TDGIS, its incoming gas transfer lines and the AGHS share a common secondary containment envelope. The design, commissioning and initial operating experience of the TDGIS are described in this paper and also in detail in [11]. The ability to allow individual beamline quadrants to operate simultaneously in different gases (deuterium or tritium) was included in the design of the TDGIS; this operational flexibility was a necessary requirement for certain D-T plasma experiments which required control of the D:T beam particle fuelling ratio while maintaining approximately constant beam energy. The resulting problem of interaction between adjacent quadrant deflection magnets, when set for different beam masses, had to be addressed and is discussed in this paper and also in [12]. Only the 160kV injector system was actually commissioned in tritium; the combination of 160kV tritium and 80kV deuterium beams is the most favourable in terms of total delivered power and also gives an acceptable balance in the relative D:T beam fuelling rates at full power (the T:D fuelling ratio was closer to 1:2 at the operational acceleration voltages and extraction currents used in practice). The option to commission the 80kV injector in tritium was retained only as a backup in case, for example, it was required to achieve satisfactory plasma D:T mixture control. As expected, it did not prove necessary to exercise this option.

The experience obtained over the different phases of commissioning and operation of the tritium neutral injector is also presented and discussed in this paper, namely: specific tritium-related commissioning simulated using deuterium, first commissioning of tritium beams, and routine tritium beam operation. Information on isotope exchange in the copper beam-stopping elements as inferred from analysis and modelling of beamline neutron emission measurements, is also presented (see also [13]). Accumulation and release of tritium in actively cooled structures exposed to high fluences of energetic particles is of importance in terms of tritium accountability, tritium content and cleanup of components, and as a potential source of contamination of the cooling water. The repair [14] of an *in vacuo* water leak in the 140/160kV beamline, which had at that stage already been operated in tritium, is also discussed. A number of safety interlock and protection systems for which credit was taken in the JET safety case documentation, relate to the neutral beam injectors and their ancillary systems; this aspect is discussed in detail in [15].

2. TRITIUM/DEUTERIUM GAS INTRODUCTION SYSTEMS (TDGIS)

2.1 Function and design features of TDGIS

The AGHS installation provides centralised facilities for D_2 and T_2 gas storage and delivery, forevacuum pumping of the torus and injectors, impurity separation and processing, cryo-distillation and gas chromatographic isotope separation. The overall system therefore operates as a closed loop, all gas recovered from the torus and neutral injector systems being re-processed and stored for re-use. The total system overview is shown in Fig.2. T_2 and D_2 gases for use in the NBI systems are stored on uranium beds in the Product Storage (PS) system of the AGHS. Gas generated from the heated uranium beds is expanded into the Gas Introduction (GI) section, from which it is further expanded into the Gas Distribution (GD) box located in the torus hall basement approximately 100m away from GI. When the pressure, as determined by the controlled uranium bed temperature, has stabilised at 0.12MPa the uranium beds are isolated and cooled. Gas contained within GI and GD is then available for expansion into either or both of the TDGIS serving the two NBI systems. GI and GD, whose internal volumes are known, are all equipped with accurate manometers and temperature sensors in order to allow the amount of gas transferred at each stage to be computed from the PVT data. The internal volume (9×10^{-3} m^3) of the pipework of GI, GD represents the reservoir of gas, at the initial pressure of 0.12MPa, available for operation between top-ups, allowing several pulses to be performed. The internal TDGIS pipework volume was 2×10^{-4} m^3; the small amount of gas contained within this volume at the end of the day had to be evacuated into the beamline vacuum system (see section 5). An additional reservoir volume was available on the deuterium branch of the system located within GI

The function of the TDGIS is to supply either D_2 or T_2 gas at a stable pre-set flow rate to each PINI over the specified time interval, to provide the means to select the particular gas in a secure way (interlocked with the beamline residual ion deflection magnet setting) and avoid gas mixing. The system consists of process pipework, pneumatically actuated on-off valves,

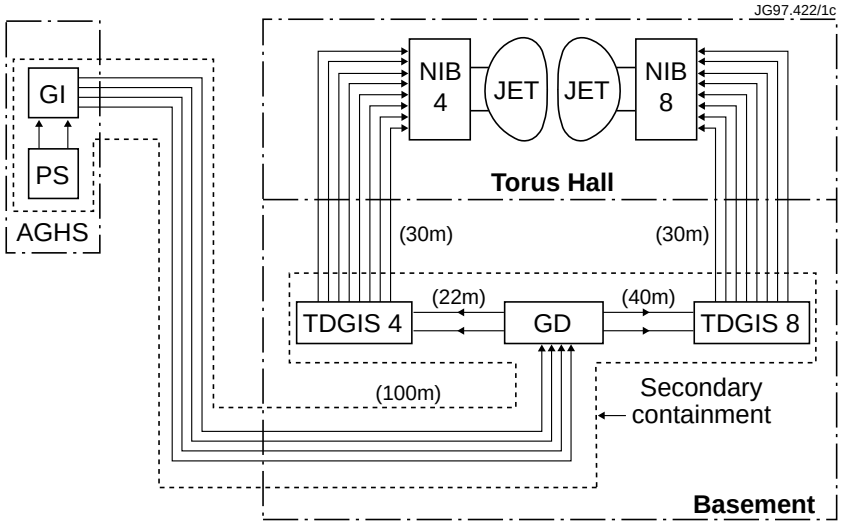

Fig.2: Interconnection line diagram of Active Gas Handling System (AGHS), Product Storage (PS) and Gas Introduction (GI); Gas Distribution (GD) and Tritium-Deuterium Gas Introduction Systems (TDGIS); Neutral Injector Boxes denoted NIB4 (80kV) and NIB8 (140/160kV).

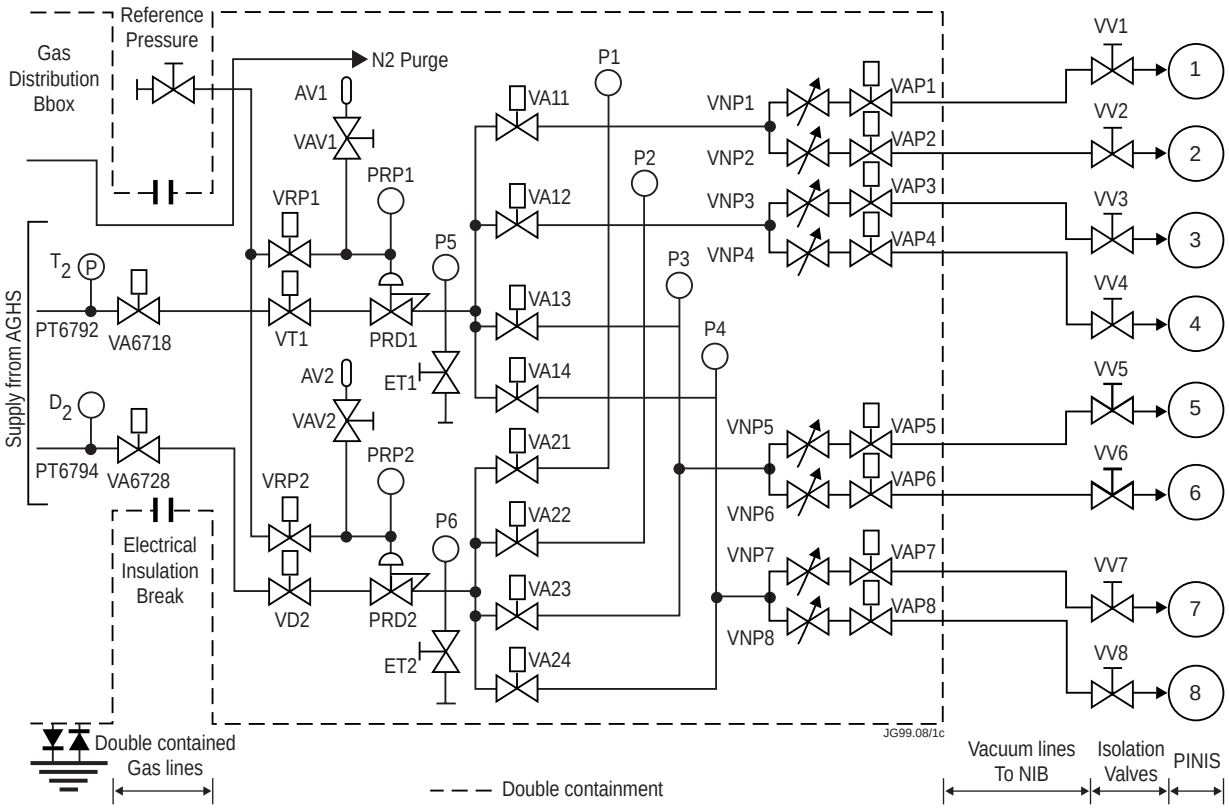

Fig.3: Schematic diagram of the TDGIS

manometers, diaphragm pressure regulators and pre-set adjustable dosing valves. The TDGIS is enclosed within a secondary containment volume which is contiguous with that of the double-containment D_2/T_2 transfer lines from the GD box and extends back to the AGHS; this volume is continuously purged with N_2 and monitored for tritium activity in operation. A schematic diagram of one TDGIS is shown in Fig. 3. Valves VA6718 and VA6728 enable the supply of T_2

and D_2 respectively, located within GD. The pressure regulators PRD1 and PRD2 are required to operate stably down to an output pressure of 40kPa; this allows for a sufficient input pressure drop during the pulse to meet the requirements of long NBI pulses (up to 10s beam duration) whilst allowing the combined GI+GD volume to be minimised, in order to limit the amount of potentially releasable T_2 gas, i.e. not held on the uranium bed, at a given time. The pressure downstream of the regulators is monitored by gauges P5 and P6, and is maintained at the constant pressure of the gas enclosed on the reference side of the diaphragm. This gas was chosen to be ^{3}He and D_2 for the tritium and deuterium branches respectively of the system to avoid problems of residual ion dumping if the regulator diaphragm were to rupture, and the regulator gas were to enter the ion source gas feed. The needle valves VNP1-8 were adjusted during commissioning to provide the required flow rate in the range of 2.5-3Pa.m^{3}s^{-1} at 40kPa. The reservoirs AV1 and AV2 provide sufficient volume to prevent fluctuations in the reference pressure as the diaphragm deflects. The selection of deuterium or tritium for a beamline quadrant (i.e. pair of PINIs) is effected via the manifold selection valves VA11-VA24 independently for each quadrant. Operation of the tritium selection valves is via keyswitches. The identity of the gas being used on each beamline quadrant is also entered by the operator into supervisory software running on the neutral injection sub-system control computer. The key-switch and software selection are automatically checked for consistency before every pulse, this is particularly important since the software sets the residual ion deflection magnet current according to the selected isotope. The possibility of gas mixing is prevented by first evacuating the manifold volume to the beamline; an interlock prevents operation of the selection valves if the pressure is >100Pa. The control system ensures that operation of T_2/D_2 selection valves on a given quadrant is mutually exclusive. The output valves VAP1-8 are timer controlled and are opened simultaneously with the inlet valves VT1 and VD1, and are interlocked with the vacuum isolation valves VV1-8 on the beamline in order to ensure the output lines, which form part of the beamline vacuum envelope and therefore do not have any secondary containment, do not become pressurised with T_2 at any time. The valves ET1 and ET2 were only used for leak testing and commissioning, and remained capped during normal operation. The TDGIS control system provided fail-safe permit signals to the beamline Central Interlock and Safety System and the Fast Beam Interlock System in order to inhibit beam extraction in the event of any abnormal TDGIS operating condition [15].

2.2 Construction and commissioning of TDGIS

The TDGIS was assembled under clean conditions using UHV quality fittings and radiographed welds then vacuum leak-tested and pressure leak-tested. A full functional test of all instrumentation was also carried out before *in-situ* installation. The TDGIS secondary containment was fabricated and certified as a pressure vessel up to 1.1MPa overpressure, and built in two parts to facilitate separation for internal access without breaching the primary process containment. The arrangement of the process pipework etc. and secondary containment envelope is shown in

Fig. 4. All pneumatic and electrical connections to the internal components were via vacuum-quality feedthroughs in the pressure vessel. The output gas lines, under beamline vacuum, were sized at 25mm i.d. such that the time constant for filling and emptying their internal volume over the required length of about 30m would be sufficiently short to minimise the quantity of unused gas. Following *in-situ* installation, the internal pipework was again vacuum and pressure-tested and the reference pressures were initially set to 40-45kPa on both the deuterium and tritium pressure regulators. The needle valves were set up to give a nominal flow of 2.5Pa.m^{3}s^{-1} using a temporary local D_2 supply. The connection to the transfer lines from GD were then made and vacuum leak-tested together with the output gas lines. The secondary containment was at this stage left open to facilitate further adjustments of the gas flows in the light of experience operating the PINIs from the TDGIS in deuterium.

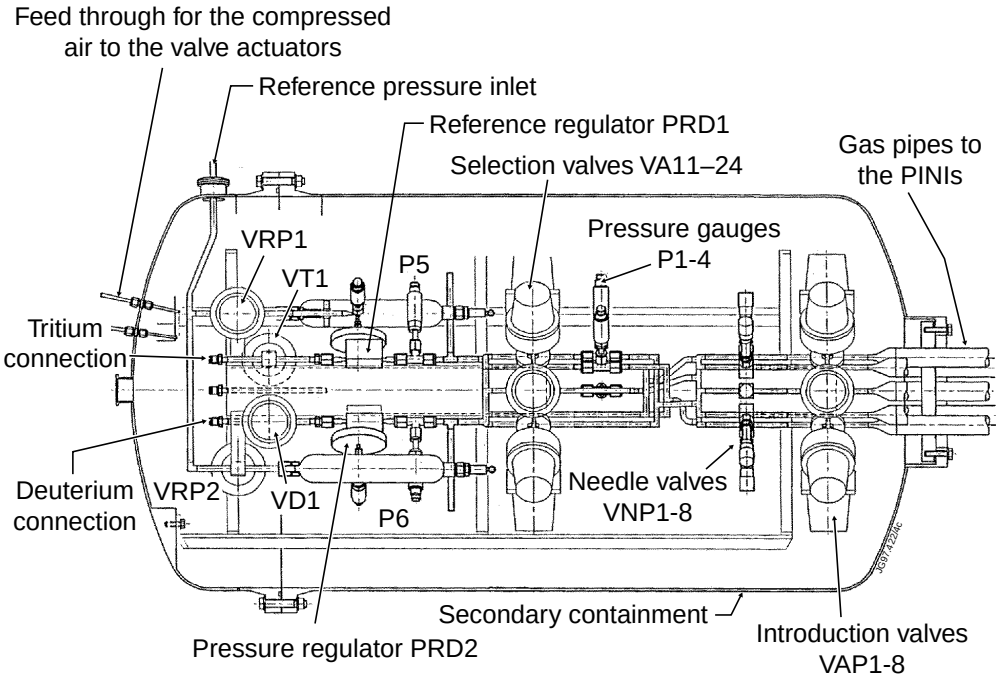

Fig.4: Physical arrangement of the TDGIS components

3. PREPARATORY COMMISSIONING OF NEUTRAL INJECTORS FOR TRITIUM OPERATION USING DEUTERIUM

After initial commissioning of the TDGIS as described in the previous section, an extended period of routine operation of both NB injectors using deuterium supplied by the AGHS/TDGIS took place. Operating procedures were rehearsed and refined, including accounting of all gas transfers using PVT measurements and re-generation of the NB cryo-pumps and recovery of the re-generated gas by the AGHS. Some operational difficulties were encountered and eliminated during this period. The most serious was the tendency for the pneumatically operated on-off valves to develop leaks across their sealing surfaces after a relatively small number (100s) of cycles; this was unacceptable since it could lead to mixing of deuterium and tritium. The valves

were initially specified to be of an all-metal (bellows, stem and seat) construction. After a detailed investigation it was shown that the stainless steel valve seat was being damaged by off-centre contact with the stellite tip of the inadequately supported stem, under the very large sealing force required. Therefore the TDGIS had to be removed and new valves fitted which incorporated a Vespel© stem tip; radiography on the new welds and local vacuum leak/pressure testing on the internal pipework was again carried out.

Following re-installation of the TDGIS it was necessary to repeat the *in-situ* vacuum leak/pressure testing of the primary and secondary containment. In fact, only the TDGIS serving the 160kV beamline was re-installed following re-fitting of the on-off valves, owing to problems operating the 80kV PINIs in deuterium with the TDGIS, as discussed below.

3.1 PINI operation characteristics with the TDGIS in deuterium

The TDGIS gas flows were lower than the conventional gas supply (the latter using separate feeds to the ion source and neutraliser). The single ground-potential gas feed is located close to the PINI earth-grid [10], denoted G4 in Fig. 5. For a given pressure in the accelerator (through which the gas must flow to feed the plasma source) the pressure in the source and the flow rate into it is lower than the case of separate feeds into the plasma source and neutraliser. Based on earlier results from the JET neutral beam test bed, the nominal TDGIS flow of 2.5 Pa.m^{3}s^{-1} of D_2 per PINI was chosen, compared with a total flow of 3.2 Pa.m^{3}s^{-1} of D_2 for normal operation with the conventional gas feed. The TDGIS was initially set up to provide a flow-rate of 2.5 Pa.m^{3}s^{-1} and then optimised experimentally taking into account the effects on arc efficiency, neutralisation efficiency and reliability. Arc efficiency may be defined as the ratio of extracted beam current to arc current (i.e. I_{ext}/I_{arc}) and depends on the gas pressure in the plasma source. Neutralisation efficiency describes the proportion of neutrals in the beam as it leaves the neutraliser, and depends on the line-integrated gas molecular number density between the accelerator and the residual ion deflection magnet entrance. Both arc and neutralisation efficiencies therefore depend on the gas-flow conditions.

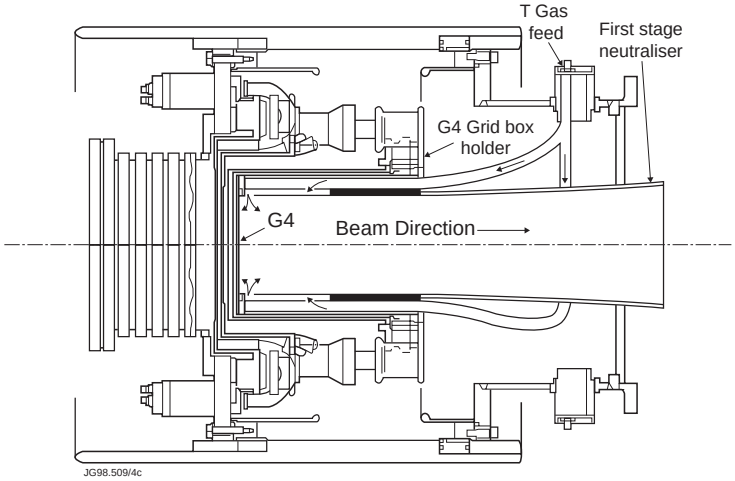

Fig.5: Horizontal cross-section of a JET PINI, showing the single gas introduction point, located just downstream of the earth-grid G4 ("grid-gas" feed)

3.1.1 160kV injector

For this injector, a deuterium flow-rate of 2.8±0.2 Pa.m^{3}s^{-1} was finally adopted; the neutralisation efficiency was then 6.5% lower than that measured using the conventional gas system for deuterium beams at 140kV. A reduction in arc efficiency was also observed, corresponding to an increase of typically approximately 24% in the arc current required to obtain a given extracted beam current, (Fig. 6). Otherwise, no particular difficulties were encountered. It may be noted that the adoption of similar reference pressures for the deuterium and tritium regulators implies a lower volumetric flow-rate for tritium. This is, however, partially compensated for by the reduced conductance for tritium flowing out of the neutraliser. The gas pressure distribution in the PINI for various operating scenarios is discussed in detail in Appendix 1.

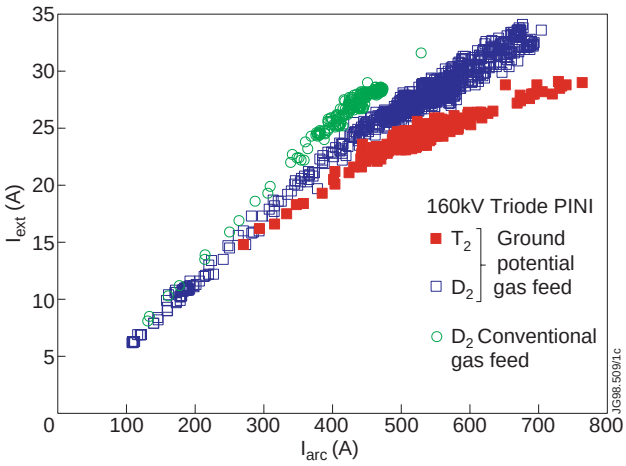

Fig.6: Arc efficiency with single ground potential gas feed (in deuterium and tritium) and with the conventional separate source and neutraliser feeds (deuterium only) for an 140/160kV triode PINI

3.1.2 80kV injector

Since the beam current is much higher on this injector, the source pressure is further reduced compared with the 160kV system, at a given gas flow-rate, leading to gas starvation and unacceptably low arc efficiency at high current (Fig. 7). The arc power supply is rated for 1200A and at the low arc efficiency observed this corresponded to a maximum extracted beam current in deuterium of about 48A, well short of the current required for optimum perveance at an acceleration voltage of 80kV. Under conditions of gas-starvation the source pressure falls by a significant proportion towards its steady-state value after the start of beam particle extraction. Since the arc parameters must be set for the required beam current in the steady-state, a substantial overshoot of the beam current was observed over a transient period of a few milliseconds while the source pressure re-equilibrated. Increasing the TDGIS flows caused several PINIs to become inoperable due to HV breakdowns, attributed to an excessive pressure in the vicinity of the accelerator grids and

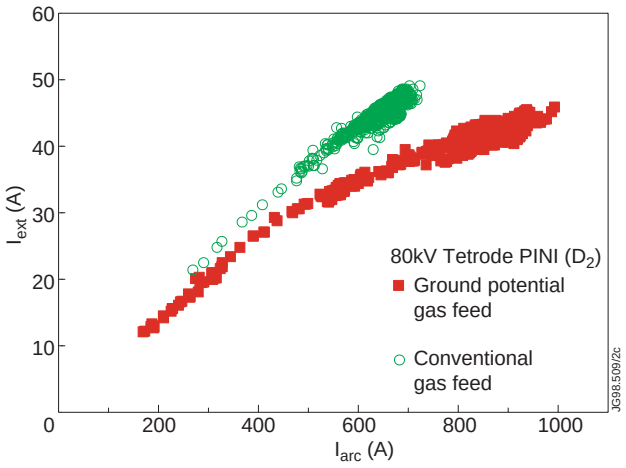

Fig.7: Arc efficiency with single ground potential gas feed (deuterium only) and with the conventional separate source and neutraliser feeds for an 80kV tetrode PINI

their support structures. These HV breakdowns were often distinctive in that they were associated with pre-cursor current excursions observed on the second (or “gradient”) grid, whose potential is derived from a resistive potential divider. The potential of this grid therefore became perturbed since the observed current excursions were significant compared with the resistor drain current of 1A. This would have the effect of substantial de-focusing of the beam optics and therefore could precipitate the hard breakdowns observed. In practice, it was not possible to achieve reliable operation above approximately 70kV, and it was decided to revert to the conventional gas handling system on this injector. A more detailed discussion of gas starvation in relation to the “grid gas feed” is given in Appendix 1.

3.2 Conditioning to 160kV

The maximum power supply current is 60A and each pair of PINIs on a quadrant of the 140/160kV injector is connected electrically in parallel. For deuterium operation the optimum perveance condition is 140kV/30A per PINI and 140kV had hitherto been the normal maximum operating voltage. The system was, however, conditioned to 160kV/37A in deuterium by energising only a single plasma source on each quadrant. Using this technique, approximately 200×0.7s duration conditioning pulses were required to obtain reliable operation at 160kV prior to commencing any operation with tritium itself.

3.3 Optimisation of gas timing

In order to reduce gas consumption per beam pulse, and hence economy of tritium usage, the duration of the gas-on period relative to that of actual beam extraction was minimised. It was, however necessary to allow a period of stabilisation of the gas flow, owing to the finite volume within the ≈30m length of vacuum lines connecting the TDGIS to the PINIs to be filled, and to allow the arc discharge to stabilise sufficiently prior to applying the beam acceleration voltage. The gas equilibration time could be reduced to 1.3s in deuterium, and the arc stabilisation time to 1.0s. It was also possible to close the TDGIS outlet valves before the programmed end of the beam pulse due to the finite amount of gas contained in the vacuum lines which has to exhaust into the PINI. If the gas were cut exactly at the programmed end of the beam pulse, this gas would be wasted. Of course, the flow rate gradually decreases once the TDGIS outlet valve closes, but analysis of the waveforms for the arc current and beam current showed that it was possible to advance the closure of the TDGIS outlet valves by as much as 0.3s. This was done by advancing the gas valve closure time, and noting the time at which the extracted current started to decay. The arc discharge current was affected much less, since it is stabilised by a feedback loop acting on the filament heater current (the arc operates in the emission-limited mode) while the decline of the extracted current reflected onset of the gas-starved condition. From such data the earliest acceptable time for cutting the gas feed was derived for each PINI.

4. COMMISSIONING OF NEUTRAL BEAM INJECTOR USING TRITIUM

No tritium was introduced into the NBI systems until all the commissioning described in the previous sections had been completed. In addition, all procedures for pumping away the gas re-generated from the beamline cryo-pumps to the AGHS had been thoroughly proved and re-hearsed [9] in deuterium by this stage. It should be noted that at this time the TDGIS for the 80kV injector system had been removed for replacement of the defective on-off valves but had not been re-installed; the decision had been made to go ahead with DTE1 with tritium operation only on the 140/160kV beamline. It was anticipated that the 80kV injector would operate only in deuterium, with gas delivered from the conventional supply; however, gas from cryo-pump re-generations still had to be collected by the AGHS for re-processing. Though never operated in tritium, the 80kV beamline was exposed to gas migrating from the torus; the beamline fast shutters [16] (designed to minimise such exposure) had to be locked open during the DTE1 campaign due to operational failures [14]. The amount of tritium contamination of the 80kV injector resulting from the lack of an operational fast shutter is discussed in section 9.2 below.

The first use of tritium in the 140/160kV beamline and associated TDGIS was with a 1% T_2/D_2 gas mixture. The low concentration mixture was progressively expanded from the AGHS into the GD box, transfer lines and TDGIS in order to confirm the integrity of primary containment of each stage of the system. This was done by monitoring the nitrogen purge gas for traces of tritium flowing in the interspace between the primary and secondary containment; no leaks were detected. After completing this stage a number of beam pulses were carried out using the 1% T_2/D_2 mixture. PINI operation with such a gas mixture did not require any specific commissioning, since at such a low tritium concentration the PINI operating characteristics are indistinguishable from those of pure deuterium. The feasibility of operating with a trace tritium concentration in deuterium was first demonstrated in the PTE campaign [17]. It may be noted that, since the residual ion deflection magnet had to be set as for deuterium operation, the 1% T_2/D_2 mixture was delivered via the *deuterium* branch of the TDGIS (since the status of the T_2/D_2 quadrant selection valves is interlocked with the corresponding magnet setting). The neutral beam injection systems are operated either in *Asynchronous-mode* (independently of the tokamak with beams impinging on the beamline calorimeter acting as beam-stop in its open position) or in *Synchronous-mode* where the beamline control is slaved to the tokamak and the beams are injected into a plasma. 1% trace tritium beams were used in both modes; the response from ^{235}U and ^{238}U fission chamber neutron detectors in Asynchronous pulses arising from beam-target reactions was useful as an approximate benchmark calibration for tracking the tritium content of beam-stopping elements (section 8) throughout the course of the DTE1 campaign. Data from the Synchronous injection of trace tritium beams was used for setting up the various tokamak neutron detectors, in particular to facilitate the correct discrimination of 2.5MeV and 14MeV neutrons from D-D and D-T reactions respectively occurring in the plasma [18].

4.1 Asynchronous-mode initial commissioning of 100% tritium neutral beam operation

Isotopic changeover was first performed by running a sequence of three filament-only pulses without gas present and then two arc-only pulses on each PINI in tritium. No increase of vacuum base pressure was observed which could be attributed to traces of ^{3}He and which might have been present due to β-decay of T. The arc struck 300ms later than in deuterium, attributed to longer gas transit time through the ~30m pipework between the TDGIS and PINIs, necessitating adjustment of the TDGIS valve timing. The first beam pulses were of 0.3s duration (with deflection magnets energised) and were carried out at 120kV. The arc parameters were set assuming the same arc efficiency as deuterium, and the same value of normalised perveance (defined by the quantity $I_{ext}A_g^{1/2}/V_{acc}^{3/2}$). Having checked the beam profiles on the beamline calorimeter, the pulse length was increased to 0.7s and a three-point perveance scan carried out by varying the beam current at constant acceleration voltage; only a slight adjustment to the arc current relative to the scaled deuterium value was required since the arc efficiency for tritium was indeed similar to deuterium at ~17A extracted current (the approximate perveance-match condition at 120kV). Eleven pulses were then expended on conditioning to higher voltage in tritium, achieving 157-160kV on six PINIs, the remaining pair achieving 140kV reliably. This stage was achieved one day following first admission of 100% tritium into the TDGIS. After further conditioning a perveance scan was obtained at 150kV on all PINIs, followed by conditioning to 160kV at optimum perveance. The arc efficiency was lower for tritium compared with deuterium for >25A extracted current; this can be understood quantitatively from the data given in Appendix 1, Table 1.1. The trend of reduced arc efficiency in tritium as the extracted beam current was increased is illustrated by the data in Fig. 6; however, the reduction observed was acceptable and the beam current required to maintain the perveance-matched condition could easily be obtained merely by increasing the arc current sufficiently. The expected scaling of the beam current from deuterium to tritium, implied by maintaining the same value of normalised perveance, is verified by the data in Fig. 8 which shows the beam profile gaussian 1/e width for both D^0 and T^0 beams, as determined from the calorimeter thermocouple array data, plotted against the normalised perveance. This result suggests that the relative fractions of the atomic and molecular ions in the extracted beam must be roughly similar in the tritium and deuterium cases such that the average beam ionic mass scales approximately $\propto A_g$. The small increase in normalised perveance for tritium suggests the monatomic ion fraction may be slightly higher than for deuterium. The slight reduction in beam profile width is probably due to the higher acceleration voltage. The similarity of beam profile shapes for D^0 and T^0 beams is illustrated by the profiles shown in Fig. 9. Comparison of the neutral beam power density for D^0 and T^0 beams, as measured at the calorimeter and normalised by the total extracted beam power $V_{ext}I_{ext}$, corresponded to the result expected assuming only the change in the values of the

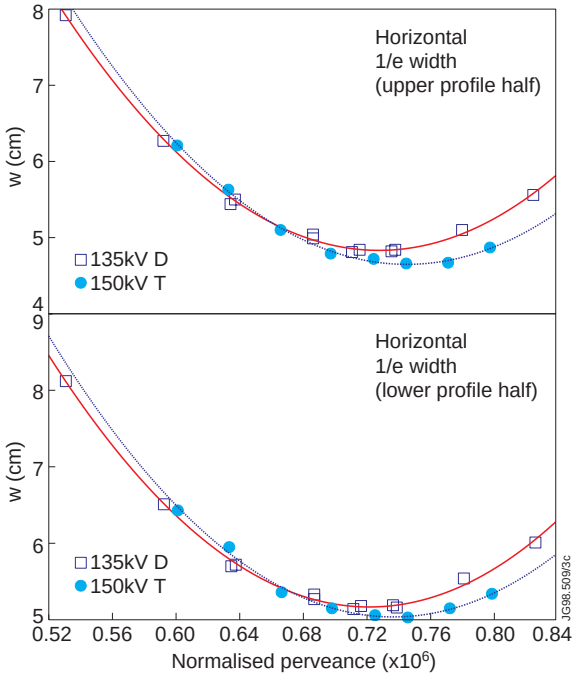

Fig.8: Horizontal beam 1/e width (from gaussian fit to profile at calorimeter) plotted versus normalised beam perveance ($I_{ext}\ A_g^{1/2}/V^{3/2}$) for deuterium and tritium beams at 135kV and 150kV respectively

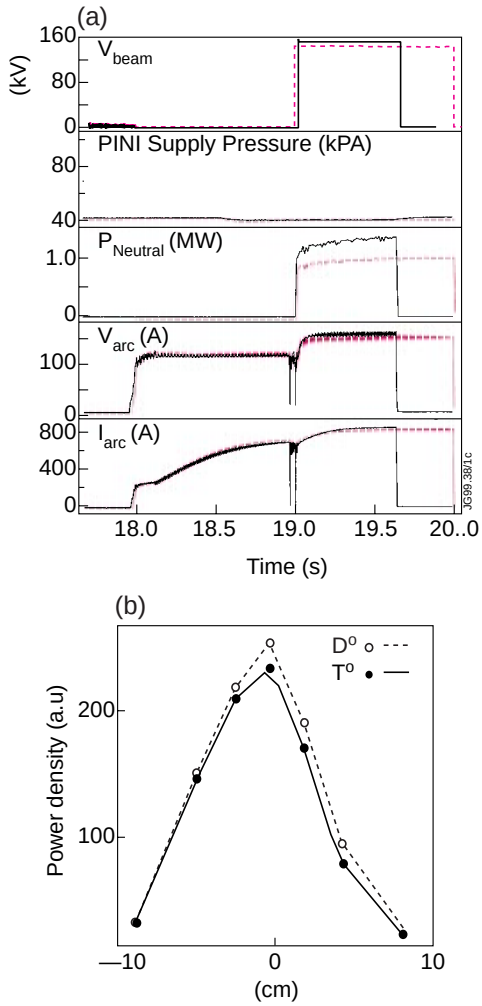

Fig.9: (a) PINI waveforms for tritium (solid lines) and deuterium (dashed lines) (b) Calorimeter profiles of tritium neutral beam (at 155kV) and deuterium neutral beam (at 140kV)

charge-changing collision cross sections(1) σ_{10} and σ_{01} on scaling from deuterium to tritium. This result implies a similar neutraliser target thickness for tritium as that previously established for deuterium, as assumed in the data summarised in Table 1 and in the computation of the power delivered to the JET plasma in subsequent Synchronous-mode operation.

4.2 Synchronous-mode initial commissioning of tritium beam injection into plasma

Before proceeding to full pulse length and power, the beam alignment, power loading on beam scrapers and drift-duct pressure evolution were all assessed by short injection pulses at reduced power. The first test pulse was at 120kV (the same neutral beam power as the standard 140kV deuterium case). Since beam power from different PINIs can overlap on some beamline components, such as beam-scraper elements in the drift-duct region, the timing of the PINIs on each

[1] For the processes of the type $H^+_{fast} + H_2 \xrightarrow{\sigma_{10}} H^0_{fast}$ + products, and $H^0_{fast} + H_2 \xrightarrow{\sigma_{01}} H^+_{fast}$ + products.

beamline quadrant was separated to allow each pair of beams to be assessed individually in the same JET discharge, using firstly 0.5s then 1s duration pulses. By scaling the measured power loadings, it was shown that a full power 160kV pulse should be within safe component limits. The process was repeated at 150kV and finally a demonstration pulse with six PINIs at 160kV and two at 150kV, energised simultaneously, was performed confirming the safe component power loadings. The entire tritium beam commissioning procedure (Asynchronous and Synchronous modes) took six operational days and used 4.71kPa.m^3 (11.6g) of tritium.

5. ROUTINE TRITIUM NEUTRAL BEAM OPERATION

After the first tritium beam commissioning had been completed, routine gas changeovers were carried out by evacuating the TDGIS output manifold prior to selecting the new gas, performing filament and arc pulses as described in section 4.1 above, then proceeding to beam extraction using the arc setpoints previously established. At the end of every operational day, all gas in the GD box, transfer lines and TDGIS was evacuated. Gas upstream of the TDGIS inlet valves (VD1 and VT1) was recovered to the AGHS uranium beds, whilst gas in the TDGIS internal volume was evacuated into the beamline prior to the nightly cryo-pump re-generation.

The only significant difficulty encountered which directly related to tritium beam operation was a tendency for the state of HV conditioning of the accelerator grids to deteriorate above 155kV slowly over the duration of the DTE1 campaign. Tritium supply inventory constraints limited the number of conditioning pulses in tritium. For reliable operation, the tritium beam energy had to be limited to 155kV. It should be noted that, for routine JET operation, no neutral beam conditioning pulses are performed between tokamak discharges.

Unfortunately, however, a component failure occurred on the 140/160kV beamline after completing the commissioning of tritium beams, during a period in which the system was set up for deuterium operation and when final preparatory deuterium plasma experiments were being conducted just prior to planned high fusion power experiments in D-T plasmas. This failure and the remedial work necessitated by it are described in detail in [16] and outlined in the following section.

6. INTERNAL WATER LEAK ON THE 140/160KV TRITIUM NBI SYSTEM AND ITS REPAIR

6.1 Detection and nature of fault

On 4 June 1997, an operational day, there were indications of an *in vacuo* water leak in the 140/160kV beamline, associated with operation of the fast shutter located between the injector and the torus (refer to Fig. 1). The presence of water was detected at an early stage by routine operating procedures using the installed residual gas analyser and Penning gauge instrumentation. The vacuum pressure at this time (with the cryo-pumps fully operational) was approximately 5×10^{-5} Pa, a factor of $\approx$100 less than the interlock trip level which would disable beam operation;

however, the normal vacuum base pressure is $\approx 10^{-6}$ Pa. Operations on this beamline were immediately suspended. The cryo-pumps were then re-generated and warmed up to ambient temperature.

6.2 Intervention to repair the tritium-contaminated beamline

The 140/160kV beamline had operated in tritium; about 11.6g had been supplied up to this time and it was assumed that up to 0.3g might be held up in beam-stopping elements. It was clear that, even after a period of de-contamination, manned entry into the neutral injector box (NIB) would require personnel to use air-fed full suits, identical to those routinely used for manned entry into the beryllium contaminated torus. These suits offer a protection against tritium inhalation of at least a factor 100 for an entire eight hour working shift. A tritium control access cabin was built to place on the top of the NIB to facilitate the suited entry of personnel and equipment. While the construction of the access cabin was taking place, approximately one week of tokamak operation took place using deuterium, in order to remove as much of the 4.4g tritium which was retained in the torus (out of 11.5g supplied as T_2 gas). In parallel, the 140/160kV NIB was subjected to moist air purging and soaking at atmospheric pressure, with pumping provided by the Exhaust De-tritiation System (EDS) of the AGHS plant via the NIB backing line. In eighteen soak/pump cycles the tritium concentration in the exhausted air fell from 33GBq.m^{-3} to 3GBq.m^{-3}. The beamline Central Support Column (CSC) (refer to Fig. 1), then had to be removed to gain access to the fast shutter mechanism, the expected probable location of the leak. Due to its tritium contamination, the only suitable repository for the CSC was in the NIB of the 80kV beamline which had at that time been exposed only to very low levels of tritium migrating from the torus, and such exposure had been minimised, since, up to that time, the fast shutter had been used in every Synchronous-mode pulse; it was estimated that only 0.2g T_2 equivalent had ingressed and most of this would have been re-generated from the cryo-pump. It was thus feasible to store the CSC of the 80kV beamline in the JET Assembly Hall. This CSC was bagged, sealed and ventilated to a monitored stack. Twenty days after the isolation of the 140/160kV beamline the access cabin was placed in position on the NIB which was continuously ventilated by the EDS at 250m^{3}hr^{-1}. Having removed the major source of outgassing (the CSC carrying most of the beam-stopping elements) the tritium concentration dropped quickly to less than 100DAC[(2)] in the NIB thus permitting suited personnel entry. The other NIB, now sealed and containing the heavily tritium contaminated CSC, was occasionally pumped by EDS. Tritium outgassing from the displaced CSC in the Assembly Hall was, as expected, negligible and well within stack discharge limits. Twenty two days after initial isolation, suited entry to the 140/160kV NIB was effected and the leak identified as a failure of a convolution in a stainless-steel flexible hose cooling water connection to one of the fast shutter doors. Because this failure was the third of its kind

---

[2] Derived Air Concentration. 1DAC ≡ 0.8MBq.m^{-3}.

experienced, the leak was repaired in solid piping and the shutter doors permanently locked open. Fifty-six days after initial isolation, both NIBs were restored to normal vacuum conditions and then re-commissioned. As a precaution, the fast shutter of the 80kV beamline was also locked open in order not to flex its hoses and therefore reduce the likelihood of a further similar failure.

7. COMPENSATION OF INTERACTION BETWEEN ADJACENT ION DEFLECTION MAGNETS TO PERMIT SIMULTANEOUS DEUTERIUM/TRITIUM BEAM OPERATION

7.1 Saturation effects in JET beamline deflection magnets

In each quadrant of the JET neutral injection systems, one residual ion deflection magnet bends the un-neutralised ions from two PINIs onto one Full-Energy Ion Dump (FEID). The FEIDs are equipped with thermocouple arrays which monitor the incident beam power footprint, and in particular allow the position of the footprint in the bend-plane to be established accurately. A schematic diagram of one quadrant is given in Fig. 10.

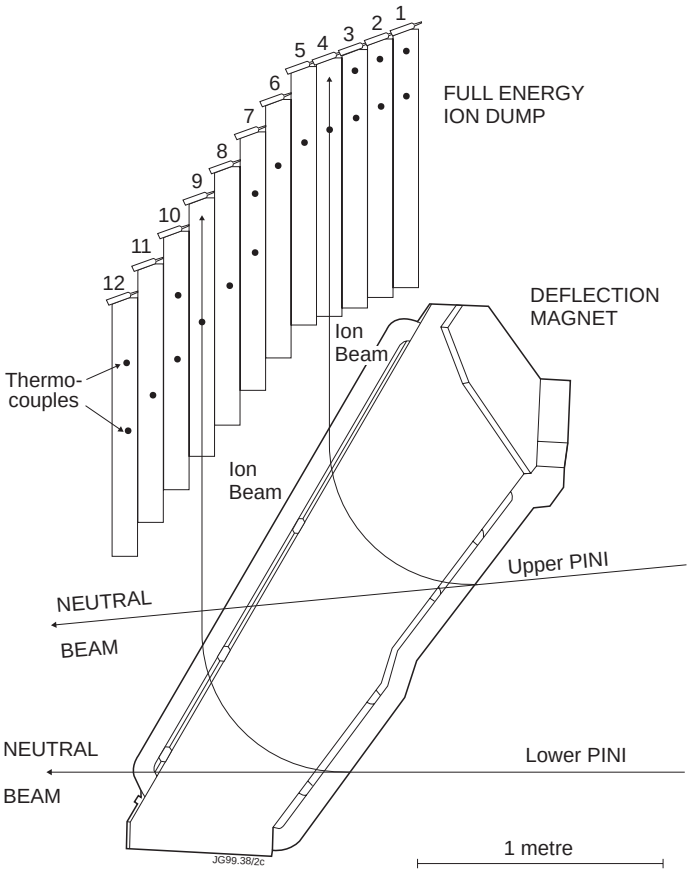

Fig.10: Beamline quadrant, showing residual ion deflection magnet, full energy ion dump, thermocouple instrumentation and beam particle trajectories

Early measurements in the NB Test Bed [19] of the bending power of the deflection magnet demonstrated a non-negligible influence from the magnets located in the adjacent quadrants. This effect is due to mutual exchange of magnetic flux between adjacent magnets which is of unequal magnitude when the magnet excitation currents differ (the effects cancel for similar excitation currents in adjacent magnets). This is a result of partial saturation of the iron circuit, in particular at the yokes which complete the magnetic circuit at the ends of the polefaces; the effect is illustrated schematically in Fig. 11. When operated at the current required for 140kV deuterium operation ($\approx$ 550A), the effect on bending power is clearly evident as a shift of the power footprint observed in the FEID thermocouple data depending on the energisation status of the magnets in adjacent quadrants. The FEID consists of a set of twelve pairs of straight “hypervapotron” elements [8] with each pair inclined to

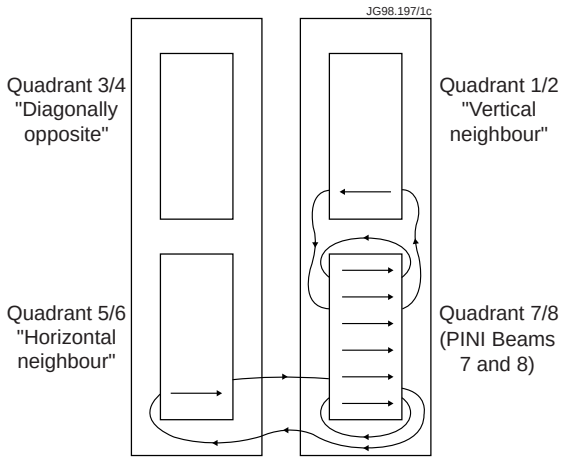

Fig.11: Schematic representation of the four quadrant deflection magnets, indicating the flux leakage from the lower right quadrant (denoted 7/8) into the neighbouring magnets

form a narrow vee; the data in Fig. 12 indicate a displacement of the deflected beam profile corresponding to about one element width, which is about the maximum acceptable shift. It was realised that the effect could not be ignored at the higher magnet currents (≈800A) required for 160kV tritium beams. Moreover, the magnet currents cannot be made equal when adjacent quadrants are operating in different gases. The TDGIS was, however, especially designed to permit mixed D_2/T_2 operation, a vital feature necessary to carry out experiments such as demonstration of the effect of alpha particle self-heating in DT plasmas [20]. Therefore, a method of correcting the magnet set-point was required in order to permit the use of different gases on adjacent beamline quadrants.

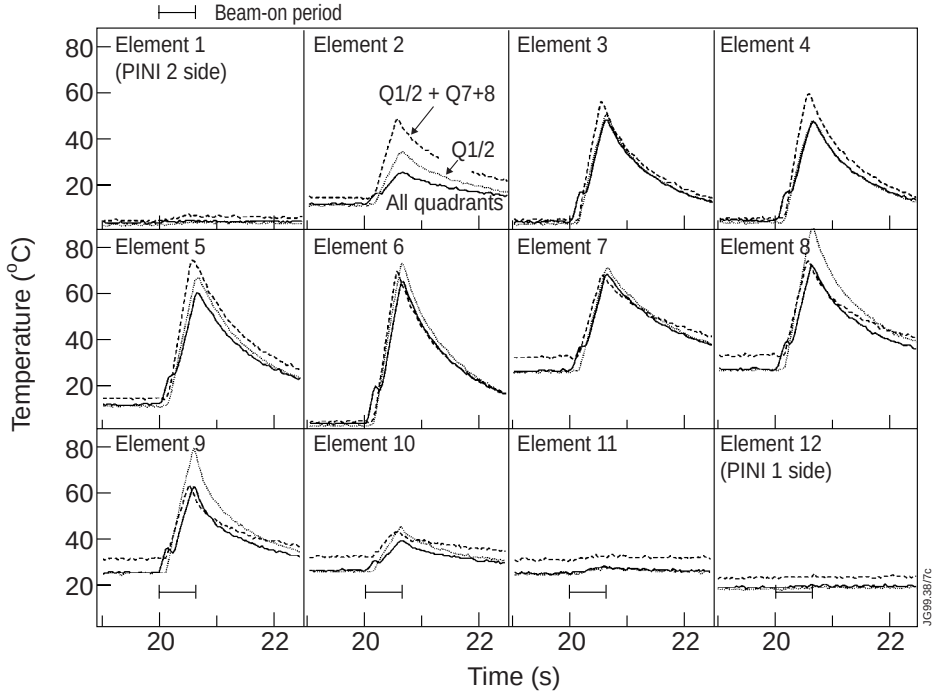

Fig.12: Time traces of the thermocouple responses of the full energy ion dump in quadrant 7/8 for a 1s 140kV deuterium beam, for a magnet current setting of 550A. Solid lines: all four quadrant magnets energised. Dashed lines: only the active magnet energised. The period of beam extraction is indicated. Note that for short beam pulses, the temperature does not reach steady-state and the observed $\Delta T \approx$ local power density.

7.2 Model for the magnet interaction

The influence of a vertical, horizontal or opposite neighbouring magnet carrying a current I_V, I_H or I_O respectively on the bending power of a given magnet carrying a current I is defined by that correction ΔI which must be added to I to restore the bending power observed when all neigh-

bouring magnets are de-energised. It was assumed that the contributions of the different neighbours could be added linearly; this is not necessarily the case physically but as shown in section 7.3, the assumption appears to be reasonably valid. From analysis of the earlier neutral beam test bed data and beamline data from previous helium operation [12] (in which the deflection magnet currents had been allowed to differ by only ± 10%) it was concluded that the existing magnet calibration model $I(V_{ext},A_g)$ was accurate up to the required ≈800A providing the horizontally and vertically adjacent magnets were energised at the same current ($I = I_V = I_H$), while the influence of the diagonally opposite quadrant could be neglected. The following form of expression is consistent with these observations, is linear, and may be considered as a measure of the difference between the magnetic flux leaving the magnet and the flux from its neighbours which leaks into it:

$$\Delta I\ (I_V, I_H\ , I) = F_V(I_V, I) - F_V(I, I) + F_H(I_H, I) - F_H\ (I, I) \qquad (1)$$

The corrected setpoint would then be given by:

$$I_{setpoint} = I(V_{ext},A_g) + \Delta I(I_V, I_H\ , I) \qquad (2)$$

In particular, equation (1) has the desired property that $\Delta I = 0$ for the condition $I = I_V = I_H$. It may be noted that the uncorrected magnet calibration $I(V_{ext},A)$ increases more quickly than $V_{ext}^{1/2}$ for I>≈500A, also attributable to magnetic saturation [21]. A further simplification of the parametrisation is to assume that the flux-leakage depends on I in the same way for all neighbours; this allows equation (1) to be written in the form:

$$\Delta I\ (I_V, I_H\ , I) = f_*(I) \times [\ f_V(I_V) - f_V(I) + f_H(I_H) - f_H(I)\ ] \qquad (3)$$

This simplification reduces the problem to that of establishing a set of three one-dimensional functions, rather than having to scan a multi-dimensional parameter space.

7.3 Measurement of magnet interaction

A series of measurements was carried out on the 140/160kV beamline in Asynchronous-mode in order to establish the functions f_*, f_H and f_V. Because of limited experimental time, only two values of I were chosen, 551A (for 140kV D^+) and 780A (for 156kV T^+), while I_V, I_H were varied between 0 and 875A. Due to the symmetry of the problem, it was only necessary to perform the measurements of bending power in one quadrant using the isotope and voltage corresponding to the two chosen values of I respectively. In practice, the 140kV D^+ measurements were performed in quadrant 1/2, and the 156kV T^+ data in quadrant 7/8 (in the nomenclature of Fig. 11). No beams were run in the neighbouring quadrants, only the magnets were energised. A reference pulse was first obtained with $I = I_V = I_H$. Then I_V and I_H were separately varied from I in small increments. The value of I was adjusted in such a way to reproduce the reference profile on the FEID. In this way, ΔI was obtained to 1-2A accuracy.

7.4 Derivation of model curves for magnet interaction from measurements

The result of the above measurements represented the horizontal and vertical magnet interaction $F_H(I_H, I)$ and $F_V(I_V, I)$ at two values of I and many values of I_H and I_V. It was then necessary to find one dimensional functions f_*, f_V and f_H that fitted both values of I and which could also be used for interpolation. A suitable choice of function f_* was found to be $f_* = (I/I_{CAL})^{\gamma}$ where I_{CAL} is taken as the value of I at which a measurement is available, e.g. 780A. The magnet correction formula can then be written as:

$$\Delta I = [\ I(V_{ext}, A) / I_{CAL}\ ]^{\gamma} \times [\ f_V(I_V) - f_V(I) + f_H(I_H) - f_H(I)\ ] \qquad (4)$$

for I_{CAL} = 780A and γ = 1.5, and where the functions f_H and f_V are given in Table 2. It may be noted that since equation (4) involves taking a difference between the functions f_V and f_H, the zero of the functions can be defined to be at any arbitrary argument; this was taken as 780A for convenience. A comparison of the measured optimum magnet setting with the predictions of equation (4) is shown in Fig. 13, and it can be seen that the results are satisfactory. Additional verification was provided by a

Table 2: Correction terms for deflection magnet interaction model parametrised as equation (4)

I, I_H, I_V(A)	f_V(A)	f_H(A)
0	33	32
300	23.2	31
550	15	23
780	0	0
900	-7.8	-12

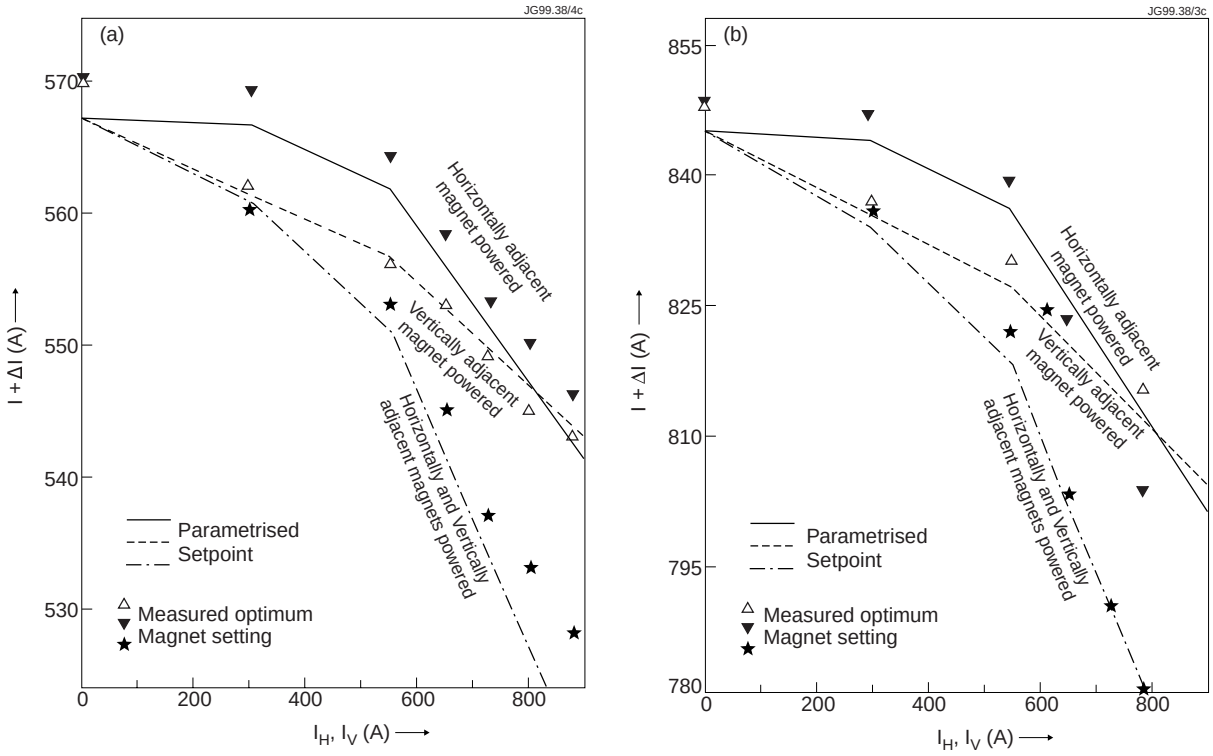

Fig.13: Magnet set-points for optimum deflection whilst the currents in neighbouring quadrant magnets are varied (a) 140kV deuterium beam (b) 156kV tritium beam. The experimental data points are compared with the parametrisation defined in equation (4) and Table 2

series of Asynchronous test pulses designed to test the model with cases which were not used in its derivation. It was especially important to verify that what had been measured in quadrants 1/2 and 7/8 also applied for quadrants 3/4 and 5/6. Permutations of 765A, 551A and 0A were run on all magnets and formula (4) was applied throughout. The FEID footprints that deviated the most from a reference shot with $I = I_V = I_H$ are shown in Fig. 14.

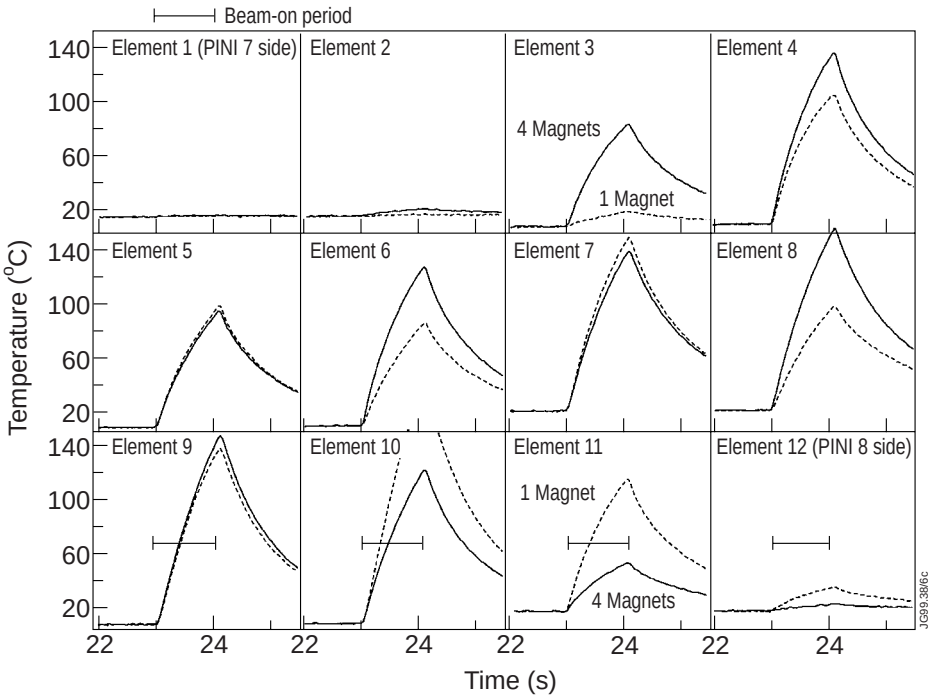

Fig.14: Time traces of the thermocouple responses of the full energy ion dump in quadrant 1/2, for corrected magnet set-point using equation (4). Solid lines: a reference pulse with all magnets energised at 765A. Dotted lines: only the active magnet is energised; the profile is slightly wider. Dashed lines: quadrant 7/8 also energised at 765A; the footprint is only slightly shifted (c.f. Fig. 12)

8. BEAM-TARGET REACTIONS AND ISOTOPIC EXCHANGE IN COPPER BEAM-STOPPING ELEMENTS

8.1 Neutron measurements

Two neutron detectors, a ^{235}U and a ^{238}U fission chamber, located on the JET machine adjacent to one side of the 140/160kV beamline, formed part of an extensive array of similar detectors used for diagnosing the plasma neutron emission. This particular pair of detectors was in addition connected to the neutral injection data acquisition system in order to permit measurements of neutrons resulting from beam-target reactions in beam-stopping elements in Asynchronous-mode beam pulses. In Synchronous-mode injection, neutrons from plasma reactions completely dominate the measured signals, and no useful information can be derived about beam-target reactions. The objective of the measurements was to determine the pulse to pulse evolution of the beam-target D-T reaction rate in a given component over a long period of time (during which there were intervals of beam operation) in each of the hydrogen isotopes. In order to relate the

raw data from the fission chambers to the beam-target reaction rate, it was necessary to consider the following factors: (i) dead-time correction of the raw count rate (ii) the relative sensitivity of the ^{235}U and a ^{238}U fission chambers for 2.5MeV and 14MeV neutrons (iii) location of the detectors with respect to the source of the neutrons. When the preceding factors were properly taken into account, it was possible to fit very satisfactorily to the data, a model which describes the evolution of the isotopic composition of hydrogenic species driven into the Cu material of the beam-stopping elements. The model is described in section 8.3, and the results give very useful information on the build up of tritium and its subsequent de-sorption during the 'cleanup' phase of beam operation in deuterium and hydrogen.

8.1.1 Instrumental dead-time correction

Dead-time corrections to the measured count-rates are necessary since there is a finite time τ_{dead}, after a count is measured, during which the detector remains insensitive to a subsequent event. Due to the random nature of the events (i.e. Poisson statistics) the dead-time correction to be applied to the measured frequency $F_{measured}$ in order to obtain the actual frequency F_{actual} can be expressed as:

$$F_{actual} = F_{measured} / (1 - \tau_{dead} . F_{measured}) \quad (5)$$

The dead-time of the neutral injection data acquisition electronics was determined in a Synchronous-mode pulse using the data measured during the decay of neutron emission from the plasma after a short tritium beam pulse. $F_{measured}$ was compared with corrected data from the same detector obtained using the JET neutron diagnostic system electronics whose dead-time had been well established; the comparison was made over several orders of magnitude and showed that a single value of $\tau_{dead} \approx 0.67\mu s$ adequately characterised the response of the neutral injection data acquisition electronics. Typical maximum uncorrected count rates were about 300kHz, whilst rates of order a few tens of Hz represented the realistic minimum as dictated by counting statistics. The ^{235}U fission chamber's sensitivity is approximately 4×10^3 times that of the ^{238}U device and this combination of neutron detectors gave a practical measurement range of about 7 decades.

8.1.2 Calibration of the ^{235}U and ^{238}U fission chambers

An approximate indication of the relative sensitivity of the ^{235}U fission chamber to 2.5MeV and 14MeV neutrons (arising from D-D and D-T reactions respectively) was obtained by comparing data from the 1% tritium beam pulses with that for pure deuterium, measured when the beam dumps were saturated with pure deuterium. A more exact interpretation of this comparison would involve taking account of the ion slowing-down distribution in the target, as described in section 8.3. The raw data, however, provided a useful simple benchmark for later comparison with data obtained during the post-DTE1 cleanup phase, being indicative of the neutron emission corre-

sponding to ≈1% residual tritium in that part of the target accessible to 140kV deuterium beams. All operation with 100% tritium beams resulted in count-rate saturation of the ^{235}U detector. Therefore, it was necessary to use the ^{238}U detector for these pulses, and in order to relate the data to measurements made with the ^{235}U detector the results were cross-calibrated during a period of deuterium operation in the cleanup phase when the neutron emission was at a level such that either detector could be used satisfactorily.

8.1.3 Dependence of detector sensitivity on location of neutron source

In Asynchronous-mode pulses, most beam-target interactions take place on the beamline calorimeter and FEID assemblies. The contributions from each of the four beamline quadrants were distinguished through the use of separated beam timing. The relative contribution from the calorimeter and ion-dumps could be estimated approximately from their relative distances from the neutron detectors. In addition, because the detectors were located to the side of the beamline, neutrons from the FEID of the quadrants on the opposite side were attenuated and moderated by having to pass through the central support column of the system (which also forms the main cooling water manifold) and through the adjacent ion-dump on the side nearest the detector; such effects were estimated to reduce the sensitivity by a factor of ≈5 for the farthest FEIDs whilst the calorimeter was not subject to these effects. Comparison of the neutron signal for quadrants on either side of the beamline implied that the neutron emission from the calorimeter dominated the measurements; this result was further supported by experiments (at reduced acceleration voltage and current) in which the residual ion deflection magnet was switched off such that all particles were incident in the calorimeter. Furthermore, the decline of neutron emission during the cleanup phase correlated much better with deuterium fluence to the calorimeter than with fluence to the FEIDs; it should be noted that over a given period of operation the fluence to the FEIDs greatly exceeds that to the calorimeter because the latter is not exposed during Synchronous-mode operation.

8.2 Evolution of beam-target neutron emission over DTE1 campaign

Large quantities of tritium, deuterium and also hydrogen were implanted into the various beamline components during the course of DTE1 and in the subsequent cleanup phase; the fluence to the different components over the two phases of the DTE1 campaign is summarised in Table 3. The first period refers to operation prior to the appearance of the internal water leak discussed in section 6, and the second period to operation following completion of the repair. The number of particles extracted from the plasma source was calculated as $N = (f_1 + 2f_2 + 3f_3)I_{ext}\Delta t$ where f_1 , f_2, and f_3 are the fractions of monatomic, diatomic and triatomic ions and Δt is the pulse length. The neutralisation efficiency for each species was taken into account in attributing the fluence to the various beamline components of each hydrogen isotope. Typical acceleration voltages for hydrogen, deuterium and tritium were 110, 140 and 155kV respectively.

Table 3: Fluence of atoms of each hydrogen isotope incident upon beamline components, over the two principal phases of DTE1 campaign. Data are expressed in Coulombs (1C = 6.24 × 10^{18} atoms)

Period	20/5/97 to 18/9/97			19/9/97 to 2/2/98		
Gas	Hydrogen	Deuterium	Tritium	Hydrogen	Deuterium	Tritium
Upstream Components	0	43047	1709	29955	83531	10864
Full Energy Ion Dumps	0	103925	3518	75241	202139	22726
Fractional Ion Dumps	0	28541	836	38768	55274	5290
Calorimeter	0	44855	3449	16723	37448	10973
Calorimeter Back Panel	0	1417	38	796	3749	469
Box Scraper	0	5678	152	3184	14988	1877
Duct Scraper	0	4259	114	2388	11241	1409
Injected to Plasma	0	51484	1427	30017	141173	17867
Total	0	283206	11243	197072	549543	71475

Data for Asynchronous-mode pulses obtained during the second phase of the DTE1 campaign are plotted in Fig. 15, relating to the lower right beamline quadrant only, for which the detector is least sensitive to the (rather small) contribution from the ion-dumps. The data is normalised according to the beam current in each pulse. The results were similar for the other three quadrants. This phase of operation was preceded by a long period of deuterium beam operation, so it is reasonable to assume that the beamline components were saturated with implanted deuterium atoms. Tritium operation was followed by a long cleanup phase (Asynchronous and Synchronous modes) when large quantities of deuterium and hydrogen were injected. The decrease in neutron rate during the cleanup phase reflects the reduction of tritium retained in the calorimeter via isotopic exchange with incoming deuterium and hydrogen atoms. The very low count during the period of hydrogen operation is attributed to small quantities of deuterium (<0.1%) contamination of the beam. The gaps in the data correspond to periods of Synchronous-mode operation. At the end of the cleanup phase, the neutron rate had decreased to within a factor two of the pre-DTE1 level.

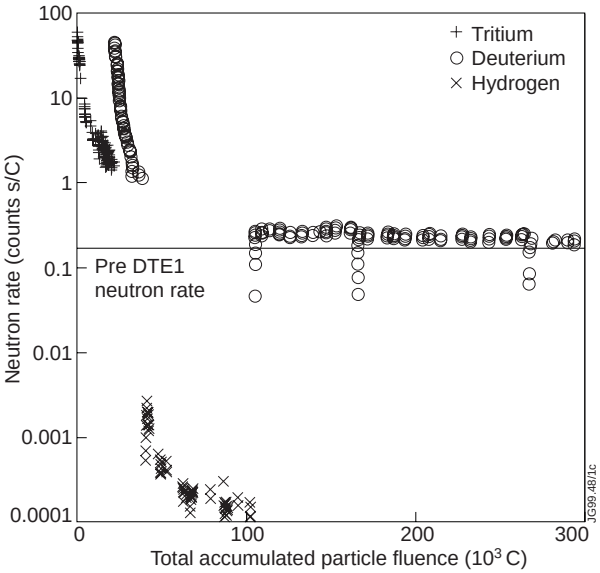

Fig.15: Neutron rate for quadrant 7/8 Asynchronous-mode pulses during the second part of DTE1

8.3 Interpretation of results using local mixing model for isotope exchange

It was previously shown in the PTE campaign [22] that the beam-target emission could be successfully described by a "local mixing model" [23,24] taking into account the stopping function of the incident particles. This model assumes that the local concentration of hydrogen isotopes cannot exceed a given saturation level (which is dependent upon temperature). When the saturation level is reached locally, one hydrogenic atom is released for every incoming atom which stops at that particular location; the probability that the released atom is of a given isotope is assumed to reflect the local isotopic mix. The displaced atom is assumed to diffuse rapidly to the surface without being trapped in any adjacent non-saturated region; at the surface it is assumed eventually to re-combine to form a molecule and to leave the material. The implantation depths are distributed according to a gaussian profile whose mean is characterised by the energy and mass of the incoming particle. For this reason account must be taken of the three velocity components in the beam arising from the acceleration of atomic and molecular ions. The details of the model and the computation of particle slowing-down and implantation profiles are described in detail elsewhere [22,25]. Slowing-down in metallic (in this case Cu) material is calculated using stopping power formulae [26]. Finally, the neutron yield is computed from the velocity-dependent cross section for the D-D and D-T fusion reactions [27] and the computed local density distribution of deuterium and tritium, again taking account of the three velocity components in the beam.

In order to compare the predictions of this model with the data, all measurements were normalised to the pre-DTE1 neutron rate (for the given beamline quadrant) and the beam current for each pulse. As discussed earlier, it was reasonable to assume that all the detected neutrons originated from reactions in the calorimeter. Figure 16 shows the comparison of the model and data for one quadrant during the second phase of the DTE1 campaign. It was assumed that the calorimeter panels were initially saturated with deuterium over the maximum range of implantation of 140kV D^+, taking into account the angle of incidence of the beams, over an area equal to that of the footprint of the beams. In the model, the particle fluence was taken to be uniformly distributed over the footprint area. In practice, the beam footprint is approximately gaussian in each dimension, however the assumption of uniformity still gives rise to a rather satisfactory description of the measured data. The acceleration energies of tritium and deuterium were subject to some variation during operation, and average voltages were used in the calculations. The changeover to deuterium indicates the start of the cleanup phase, at which time the calorimeter panels are assumed to be saturated with tritium up to the maximum depth of implantation of 155kV T^+. Figure 17 shows the results of a similar calculation for another beamline quadrant over the duration of the cleanup phase, including the period of hydrogen operation. The hydrogen beams were assumed to be contaminated with 0.1% deuterium. The local saturation density of all the hydrogen isotopes implanted in the Cu material was taken to be 20%; this value is slightly higher than that used in the PTE calculations [22,25] and it reflects the rather short pulse duration (<0.9s) and relatively low temperatures of the calorimeter elements.

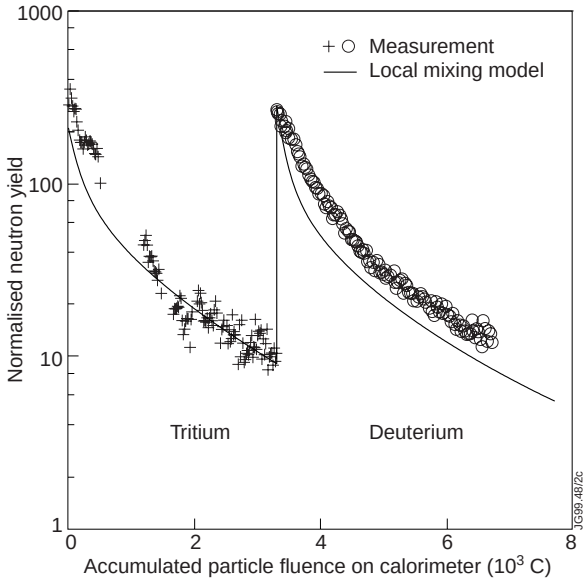

Fig.16: Normalised neutron rate for quadrant 7/8 Asynchronous-mode pulses during the second part of DTE1 with prediction from local particle mixing model

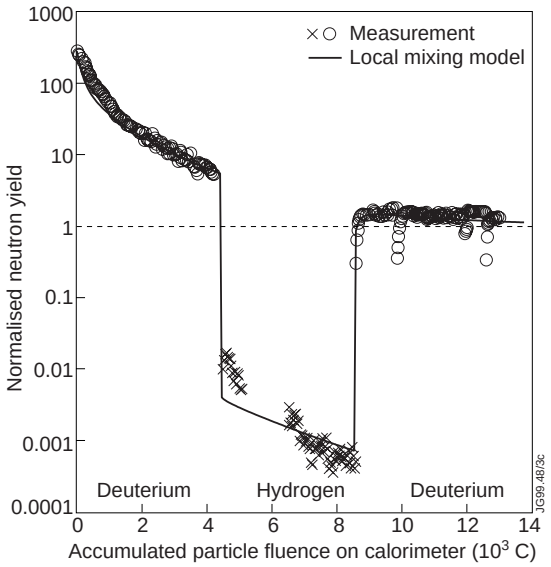

Fig.17: Normalised neutron rate for quadrant 1/2 Asynchronous-mode pulses during the second part of DTE1, including hydrogen operation, with prediction from local particle mixing model

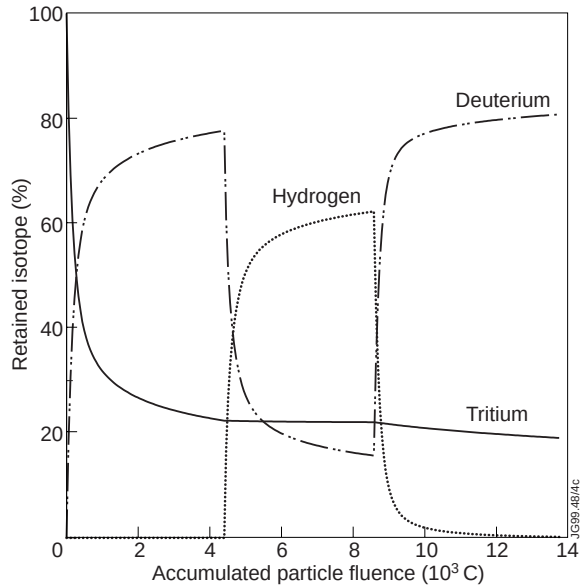

Fig.18: Retained isotopic fractions implanted into beam-stopping elements during the cleanup phase of DTE1, as predicted from the local particle mixing model

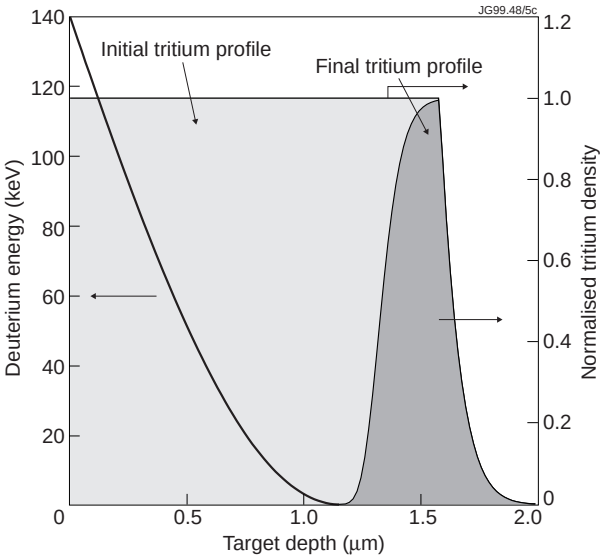

Fig.19: Tritium implantation profile at the start and end of the cleanup phase of operation, and the average range of implantation of deuterium ions as a function of incident energy

The fact that the neutron rate at the end of the cleanup phase was only slightly higher than the pre-DTE1 value does not imply that nearly all the implanted tritium was de-sorbed. This can be seen from Fig. 18 where the relative amount of retained hydrogen isotopes is plotted as a function of cumulative particle fluence and 100% refers to the condition where the saturation density is achieved up to the maximum implantation depth of 155kV T^+. Tritium which is trapped near the maximum range of implantation cannot be accessed by the lower energy lower mass

deuterium and hydrogen, as shown in Fig. 19. Furthermore, any tritium close to the maximum range of implantation of deuterium does not contribute significantly to the neutron signal owing to the low energy of deuterons which have nearly stopped, taking into consideration the energy dependence of the D-T reaction cross-section. It is therefore concluded that up to 20% of the initial tritium content of the calorimeter panels is retained at the end of the cleanup phase. In order to scavenge this residual tritium content, it would be necessary to employ deuterium beams with at least 20% higher energy than that of the originally implanted tritium, i.e. >190kV.

9. NEUTRAL BEAM PERFORMANCE AND TRITIUM USAGE DURING DTE1

9.1 Number of tritium beam pulses and power injected

The maximum power delivered by the tritium injector alone reached 10.9MW and the longest pulse duration (at 10.6MW) was 5s. In combination with the deuterium beams from the other injector a total beam heating power up to 22.3MW has been achieved. The power loadings measured on the tritium beamline components extrapolate to values which are within the normal operating limits at the maximum theoretical power for operation at 160kV given in Table 1 . This reflects the good beam optics properties observed in tritium operation, similar to the favourable characteristics observed with deuterium beams for the triode PINIs. The distribution of operating voltage for tritium beams is shown in Fig. 20. The total numbers of Synchronous-mode pulses, including only the pulses in which some tritium beams were present, and the distribution of achieved power levels for these pulses are summarised in Table 4 and Figs. 21(a) and 21(b).

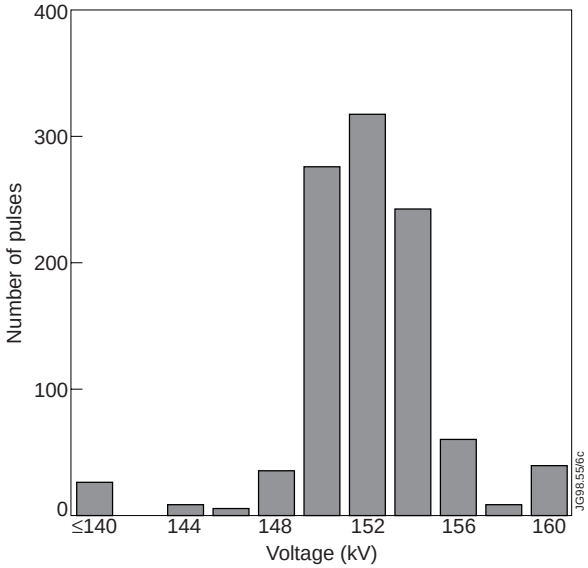

Fig.20: Distribution of operating voltages for tritium beams

Table 4: Numbers of neutral beam pulses in which tritium was used

	Asynchronous-mode pulses (onto calorimeter)	Synchronous-mode pulses (into plasma)
1% trace T_2 in D_2	3	18
100% T_2 on entire beamline	396	154
Mixed D_2/T_2 quadrants	11	6

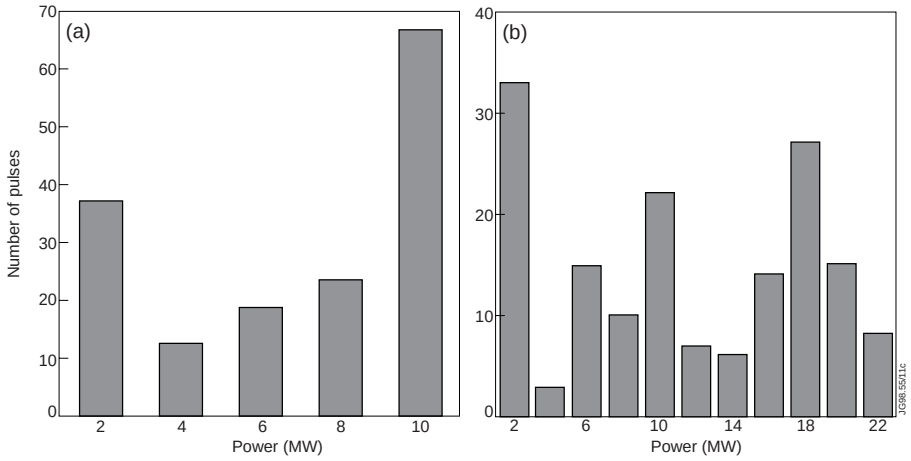

Fig.21: Distribution of achieved power levels for NB injection in which at least one PINI was operating in tritium (a) 140/160kV injector alone (4% of these pulses were with mixed deuterium/tritium quadrants) (b)combined power from both beamlines

9.2 Tritium consumption and recovery from the neutral beam injectors

PINI operation was optimised to economise on use of tritium, as described earlier, by minimising the arc stabilisation time before beam extraction and by tuning the gas valve timing. A 5s beam pulse from a 155kV/28A PINI pulse (delivering 1.4MW in the neutral beam) consumed 30Pa.m^3 tritium gas (80mg). Figure 22 shows the integrated supply and recovery of tritium for the 140/160kV injector, as measured in the AGHS plant. About 1% of the tritium supplied was injected into the plasma as neutral beam particles; it will be noted, however, that the amount recovered from the 140/160kV injection system slightly exceeds that supplied. This is due to some tritium, which had been supplied as gas to the torus, being pumped by the beamline cryo-pumps via the beamline duct [28] (since the fast-shutters were permanently open as discussed earlier). A similar effect can also be seen in the tritium recovery from the 80kV injector, which had only been operated in deuterium, from which a cumulative total of 1.9g was recovered throughout the DTE1 campaign. The post-DTE1 period of intensive deuterium operation (cleanup) was carried out in late November 1997 in order to drive out implanted tritium from dumps, calorimeter etc. and, as discussed in section 8.3, ≈80% of implanted tritium was estimated to have been removed. Tritium adsorbed or condensed (e.g. as tritiated hydrocarbons) onto the large-area,

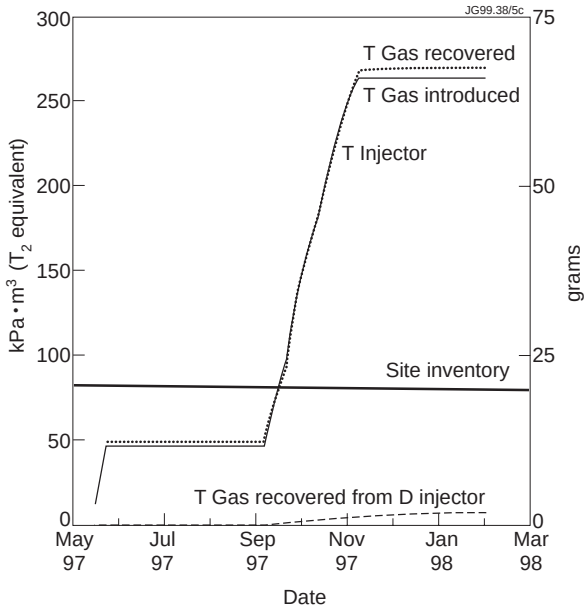

Fig.22: Cumulative tritium supply and recovery data for each JET beamline. The total site tritium inventory is shown for reference

liquid nitrogen filled, aluminium panels of the beamline cryo-pump was released by periodically warming these structures up to room temperature. The first such exercise was carried out in late November 1997, following the first part of the cleanup phase just prior to the period of hydrogen injection (see Fig.17). At the same time, the JET divertor cryo-pumps were also warmed up; since the gas recovered from the torus and the 140/160kV injector was processed in one batch, it was not possible to determine the quantity of tritium evolved from the injector alone on this occasion. Further full warming-up took place over Christmas and at the end of January 1998. In routine re-generations of the cryo-pumps during the subsequent month of operation, approximately a further 13mg of tritium was recovered *from each injector*, dominated by migration from the torus. During the 1998 shutdown, both injectors were vented to atmospheric air and, on evacuation, the 140/160kV tritium injector was found to contain 2 TBq (≈5 mg of tritium) after standing for three months.

Tritium was detected in very small quantities in water samples taken from the beamline cooling circuits. The levels steadily increased throughout the DTE1 campaign. At the end of the operational campaign (January 1998) the tritium content of cooling water from the 140/160kV injector system was 7.5MBqm^{-3}, whereas samples from the other injector were typically at the limit of detection (a few tens of kBqm^{-3}). This observation is consistent with the expectation that tritium implanted as beam particles, especially into thin-walled structures such as the PINI acceleration grids, can migrate in small quantities into the cooling channels. Based on the measured concentrations of tritium in the cooling water of the 140/160kV beamline, the total amount of tritium in the water amounted to less than 0.2μg.

In the most recent operational campaign (July - December 1998) the gas re-generated from the beamline cryo-pumps continued to be pumped and processed via the AGHS plant; typically, 1.5mg tritium was recovered from the 140/160kV injector per weekly re-generation, whilst 0.5mg was typically recovered per re-generation from the 80kV system. Since both beamlines were open to the torus vacuum for similar periods of time during operation, it may be concluded that about two thirds of the tritium still being recovered from the 140/160kV beamline at this time was attributable to isotope exchange in beam-stopping elements. Continued isotope exchange at a low rate would be expected to occur in the periphery of the beam footprint on the calorimeter and/or ion-dumps where the local fluence density is much lower than the average.

During a recent intervention (January 1999) on the 80kV beamline, the concentration of tritium in atmospheric air which had been left to stand for 10 days in the isolated system at room temperature, following venting, was ≈100DAC (corresponding to ≈67μg HTO in the air contained within the 50m^3 internal volume). The most likely source of this tritium is from the aluminium cryo-pump panels, and therefore a similar DAC level could be expected in the 140/160kV system upon venting.

10. CONCLUSIONS

One of the two JET NBI systems was successfully operated in tritium at power levels up to 10.9MW and pulse lengths up to 5s duration at typical acceleration voltages of 155kV. The NBI performance in tritium adequately met the requirements of the JET DTE1 campaign in which the objectives in terms of fusion power, amplification factor Q and demonstration of ITER-relevant plasma regimes in D-T were all achieved. A very great amount of technical experience was gained in performing all the beamline and ancillary system modifications and their commissioning using both deuterium and tritium. The only serious technical problems encountered which relate directly to systems specially engineered for tritium NB operation arose from the initial adoption of an unsuitable all-metal type of on-off valve within the tritium/deuterium gas introduction systems, and difficulties in operating the 80kV PINI beam sources using a single ground potential gas feed; this latter problem remains unsolved and will have to be addressed to permit tritium operation on the 80kV PINI at full power. The problem of operating adjacent beamline residual deflection magnets at different currents, as required for simultaneous operation of different beam sources in tritium and deuterium, was solved by deriving a universal correction model (which will also be useful for simultaneous helium/deuterium beam operation in future). The remedial work following the small fast shutter water leak required new intervention procedures to be developed for manned access in the tritium contaminated beamline; it was completed successfully, in a remarkably short time, and well within management limits for personnel radiation exposure and stack discharges. A good deal of useful data on tritium build up and release from the beamlines was obtained, and the comparison of recovered tritium from both beamlines, one of which was not exposed to tritium beam implantation but only tritium gas migrating from the torus, was in itself useful although it highlighted the value which an operational fast shutter would have afforded. The results and experience obtained in this work will be of benefit in future JET D-T operation and in the design and operation of future fusion devices with tritium.

ACKNOWLEDGEMENTS

The authors gratefully acknowledge the contribution of all members of the JET Team, especially the technical staff of Neutral Beam Heating and Fusion Technology Divisions. Without the dedicated efforts of these colleagues the work presented in this report would not have been possible.

REFERENCES

[1] The JET Team (presented by P-H Rebut), Plasma Physics and Controlled Fusion Research (Proceedings of 13th International Conference, Washington, 1990) 1(1991)27

[2] E Thompson, D Stork, H P L de Esch and the JET Team, The use of neutral beam heating to produce high performance fusion plasmas including the injection of tritium neutral beams into the Joint European Torus (JET), Phys Fluids B 5(7)(1993) 2468

[3] T T C Jones and the JET Team, High performance Joint European Torus (JET) plasmas for deuterium-tritium operation with the MkII divertor, Phys. Plasmas 4(5)(1997) 1725-1735

[4] The JET Team, Fusion energy production from a deuterium-tritium plasma in the JET tokamak, Nucl. Fusion 32(1992) 187-203

[5] M Keilhacker, A Gibson, C Gormezano, P Lomas, P R Thomas, M L Watkins, P Andrew, B Balet, D Borba, C D Challis, I Coffey, G A Cottrell, H P L de Esch, N Deliyanakis, A Fasoli, C W Gowers, H Y Guo, G T A Huysmans, T T C Jones, W Kerner, R T W König, M J Loughlin, A Maas, F Marcus, F Nave, F G Rimini, G Sadler, S Sharapov, G Sips, P Smeulders, F Söldner, A Taroni, B J D Tubbing, M G von Hellermann, D J Ward and the JET Team, High fusion performance from deuterium-tritium plasmas in JET, Nucl. Fusion (in press)

[6] T T C Jones, P Andrew, B Alper, B Balet, A Cherubini, J P Christiansen, F Crisanti, R de Angelis, H P L de Esch, N Deliyanakis, F de Luca, M Erba, A Edwards, L G Eriksson, C Frewin, P Galli, C W Gowers, G Gorini, K Günther, H Guo, N C Hawkes, T C Hender, G Huysmans, R König, K D Lawson, H Lingertat, M Mantsinen, K McCormick, A C Maas, F B Marcus, F Nave, V Parail, L Porte, F G Rimini, B Schunke, P Smeulders, A Taroni, P R Thomas, G Saibene and K-D Zastrow, Proceedings, 25th EPS Conference on Controlled Fusion and Plasma Physics, Prague, Czech Republic, Eur. Conf. Abstracts, 22C(1998)

[7] The JET Team (presented by D Stork), JET Engineering Development towards D-T operations in an ITER-like machine configuration, Proceedings of 17th IEEE/NPSS Symposium Fusion Engrg. 1(1997) 70

[8] G Duesing, H Altmann, H Falter, A Goede, R Haange, R S Hemsworth, P Kupschus, D Stork and E Thompson, JET project: Neutral beam injection system, Fusion Technology, 11(1)(1987) 163-203

[9] R Lässer *et al.*, AGHS operations and performance, Fusion. Engrg. Des., in this issue.

[10] P Massmann, H-D Falter, A J Bickley, G H Deschamps, D Hurford and E Thompson, Modifications and characteristics of the JET positive ion neutral injectors for the first tritium experiment, Fusion Technology (1992) 574-578

[11] L Svensson, A Bickley, A Browne, C D Challis, S Cox, H de Esch, H D Falter, D Godden, T T C Jones, A Konarski, D Martin and D Young, The JET active phase gas introduction systems for neutral beam injection and beamline commissioning and operation with tritium, Proceedings of 17th IEEE/NPSS Symposium Fusion Engrg. 2(1997) 1098

[12] H P L de Esch, Compensation for non-linear interaction between the JET NBI deflection magnets for simultaneous D_2/T_2 operation, Fusion Tech 1(1998) 477-480

[13] D Ciric, H P L de Esch, H-D Falter, T T C Jones and L Svensson, Isotope exchange in high heat-flux components of the JET tritium neutral beam injector, Fusion Technology 1(1998) 481-484

[14] M J Watson, A C Bell, A J Dines, F H Hurd, J G Lundquist, B J Macklin, J C Orchard and B Patel, Intervention to repair a tritiated JET neutral beam injector, Fusion Technology 1(1998) 485-488

[15] D Stork, A C Bell, A Browne, P R Butcher, C Caldwell-Nicholls, P Chuilon, S J Cox, N Davies, J A Dobbing, N Dolgetta, C Elsmore, J A How, T T C Jones, A S Kaye, Q A King, V Marchese, C Mayaux, W Obert, J Orchard, R Parkinson, R J H Pearce, L Svensson, M Wright and D Young, Systems for the safe operation of tokamaks with tritium, Fusion Engrg. Des., in this issue.

[16] M J Watson, R Haange, D Stork, R B Tivey, and D Young, A fast shutter system for the JET neutral injectors, Fusion Technology (1986) 1145-1151

[17] M Huguet, A C Bell, S J Booth, C Caldwell-Nicholls, A Carmichael, P Chuilon, N Davies, K J Dietz, F Delvart, F Erhorn, H Falter, B J Green, B Grieveson, R Haange, A Haigh, J L Hemmerich, D Holland, J How, T T C Jones, R Laesser, M Laveyry, J Lupo, A Miller, P Milverton, G Newbert, J Orchard, A Peacock, R Russ, G Saibene, R Sartori, L Serio, R Stagg, S L Svensson, E Thompson, P Trevalion, E Usselmann, T Winkel and M E P Wykes, Technical aspects of the first JET tritium experiment, Fusion Engrg. Des. 19(1992) 121-131

[18] A C Maas, P Andrew, P Coad, A Edwards, J Ehrenberg, A Gibson, K Günther, P Harbour, M G von Hellermann, D Hillis, A Howman, O N Jarvis, J F Jünger, R W T König, J Lingertat, M J Laughlin, P D Morgan, J Orchard, G Sadler, M F Stamp and C H Wilson, Diagnostic experience during deuterium-tritium experiments in JET, techniques and measurements, Fusion Engrg. Des., in this issue.

[19] H-D Falter, G Deschamps, R S Hemsworth and P Massmann, Deflection of 120kV helium beams to simulate deflected 160kV tritium beams, JET-DN-C(89)75

[20] P R Thomas, P Andrew, B Balet, D Bartlett, J Bull, B de Esch, A Gibson, C Gowers, H Guo, G Huysmans, T Jones, M Keilhacker, R Koenig, M Lennholm, P Lomas, A Maas, F Marcus, F Nave, V Parail, F Rimini, J Strachan, K-D Zastrow and N Zornig, Observation of Alpha Heating in JET DT Plasmas, Phys. Rev. Lett. 80(25)(1998) 5548

[21] L Svensson, H-D Falter, D Stork and N Traynor, Calibration of high energy beam bending magnets, JET-DN-C(90)87

[22] H-D Falter, E Thompson, D Ciric and H P L de Esch, Implantation and desorption of tritium and tritium recovery from the JET neutral beam injectors, J. Nucl. Mater. 196-198(1992) 1131-1134

[23] G Staudenmaier, J Roth, R Behrisch, J Bohdansky, W Eckstein, P Staib, S Matteson and S K Erents, Trapping of deuterium implanted in carbon and silicon: a calibration for particle-energy measurements in the plasma boundary of tokamaks, J. Nucl. Mater. 84(1979) 149-156

[24] B L Doyle, W R Wampler, D K Brice and S T Picraux, Saturation and isotopic replacement of deuterium in low-Z materials, J. Nucl. Mater. 93- 94(1980) 551-557

[25] H-D Falter, D Ciric, G H Deschamps, H P L de Esch, P Massmann and L Svensson, Hydrogen isotope exchange in the JET neutral beam injection system, Fusion Technology (1992) 481-485

[26] H H Andersen and J F Ziegler, Stopping power and ranges of ions in matter, 3(1977) Pergamon Press (New York)

[27] H-S Bosch, Review of data and formulae for fusion cross sections, IPP I/252(1990) Max-Planck Institut für Plasmaphysik, Garching, Germany

[28] P Andrew, D Brennan, J P Coad, J Ehrenberg, M Gadeberg, A Gibson, D L Hillis, J How, O N Jarvis, H Jensen, R Lässer, F Marcus, R Monk, P Morgan, J Orchard, A Peacock, R Pearce, M Pick, A Rossi, P Schild, B Schunke and D Stork, Tritium retention and cleanup in JET, Fusion Engrg. Des., in this issue.

APPENDIX 1

Gas pressure distribution in the PINI

The change in operating characteristics and, in particular, the difficulty of operating the 80kV PINI on the ground-potential “grid gas feed” can be understood more quantitatively in terms of the gas pressure distribution in the plasma source and extraction grid regions. Measurements in the JET NB Test Bed resulted in the following expression for the gas pressure distribution for a given flow F_s into the source, a flow F_n into the neutraliser and a gas flow F_{acc} extracted from the source as beam particles; the expression was found to be valid irrespective of whether the source gas flow F_s was admitted into the source itself or via the “grid gas feed”:

$$P_{grid} = A^{1/2} \{0.348(F_s-F_{acc})^{0.96} + 0.126F_n^{0.94} - 0.0336(F_s-F_{acc})^{0.6} F_n^{0.94}\} \qquad (1.1)$$

A is the isotopic mass, and the gas flows are in units of $Pa.m^3s^{-1}$ with the pressure in Pa. The non-linear character of equation (1.1) reflects the fact that the conductance along the neutraliser is pressure dependent owing to the flow regime being transitional between viscous and molecular. The conductance through the accelerator grids remains molecular and is approxi-

mately given by $C_{grid} = 1.5A^{1/2}$ m^3s^{-1} and from this the pressure drop ΔP_{grid} may be computed. For the "grid gas feed" (F_n=0), $\Delta P_{grid} = -F_{acc}.C_{grid}$, i.e. $P_{source} < P_{grid}$, because gas has to flow into the source via the grid conductance to replace the extracted beam particles. For the conventional gas feed (F_n>0), $\Delta P_{grid} = (F_{source}-F_{acc}).C_{grid}$, i.e. $P_{source} > P_{grid}$, because in this case the particle flow removed by beam extraction is less than the gas admitted directly to the plasma source. Using these results, the pressure at the accelerator grids and inside the plasma source may be calculated using typical flow rates and extracted beam currents, for both deuterium and tritium (Table 1.1). Several observations can be made from the data in Table 1.1. For the "grid gas feed" (F_n=0), the pressure in the accelerator grid region is significantly higher, for both types of PINI. The electric stress in the first acceleration gap is much higher, however, in the 80kV PINI on account of the higher perveance of the accelerator and probably explains the breakdown behaviour observed for this PINI configuration. For "grid gas feed" operation, the source pressure is lower than for the conventional source feed, and the reduced arc efficiency is a direct consequence. For tritium, the source pressure is even lower, leading to a further reduction in arc efficiency, as observed in section 4.1. Finally, given that the 80kV PINI was difficult to operate in deuterium on the "grid gas feed", it is likely that proper operation of this PINI in tritium would pose serious difficulties; further investigations into this aspect would be required before attempting such operation in future.

Table 1.1: Calculated gas pressure in the plasma source and in the vicinity of the PINI earth grid for various gas flow rates and extracted beam currents

CASE	F_{acc} $Pa.m^3s^{-1}$	C_{grid} m^3s^{-1}	F_s $Pa.m^3s^{-1}$	F_s-F_{acc} $Pa.m^3s^{-1}$	F_n $Pa.m^3s^{-1}$	ΔP_{grid} Pa	P_{grid} Pa	P_{source} Pa
140kV/30A D^+	0.48	2.1	1.2	0.72	2.4	0.34	0.68	1.0
140kV/30A D^+	0.48	2.1	2.8	2.3	-	-0.23	1.1	0.88
160kV/30A T^+	0.46	1.7	2.2	1.7	-	-0.27	1.0	0.76
120kV/17A T^+	0.30	1.7	2.2	1.9	-	-0.17	1.1	0.94
75kV/50A D^+	0.73	2.1	1.4	0.67	2.1	0.31	0.62	0.93
75kV/50A D^+	0.73	2.1	2.8	2.1	-	-0.35	0.99	0.64
85kV/50A T^+	0.71	1.7	2.2	1.5	-	-0.41	0.89	0.48